# TALENs Mediate Efficient and Heritable Mutation of Endogenous Genes in the Marine Annelid *Platynereis dumerilii*

**Stephanie Bannister,*,†,[1] Olga Antonova,*,† Alessandra Polo,*,† Claudia Lohs,*,[2] Natalia Hallay,*,† Agne Valinciute,*,† Florian Raible,*,†,[1] and Kristin Tessmar-Raible*,†**

*Max F. Perutz Laboratories and †Research Platform "Marine Rhythms of Life," University of Vienna, 1030 Vienna, Austria

**ABSTRACT** *Platynereis dumerilii* is a marine polychaete and an established model system for studies of evolution and development. *Platynereis* is also a re-emerging model for studying the molecular basis of circalunar reproductive timing: a biological phenomenon observed in many marine species. While gene expression studies have provided new insight into patterns of gene regulation, a lack of reverse genetic tools has so far limited the depth of functional analyses in this species. To address this need, we established customized transcriptional activator-like effector nucleases (TALENs) as a tool to engineer targeted modifications in *Platynereis* genes. By adapting a workflow of TALEN construction protocols and mutation screening approaches for use in *Platynereis*, we engineered frameshift mutations in three endogenous *Platynereis* genes. We confirmed that such mutations are heritable, demonstrating that TALENs can be used to generate homozygous knockout lines in *P. dumerilii*. This is the first use of TALENs for generating genetic knockout mutations in an annelid model. These tools not only open the door for detailed *in vivo* functional analyses, but also can facilitate further technical development, such as targeted genome editing.

MANY fascinating biological phenomena, of which we have little to no molecular understanding, are observed in organisms outside of those that constitute conventional molecular model systems. An interesting system that has re-emerged in recent years as model for chronobiology and evolutionary studies is the marine polychaete worm *Platynereis dumerilii* (Annelida, Lophotrochozoa). However, in *Platynereis* and other emerging model systems alike, dissecting gene function *in vivo* remains challenging.

*Platynereis* is slowly evolving, compared with other more conventional molecular model protostomes such as *Caenorhabditis elegans* and *Drosophila melanogaster* (Raible *et al.* 2005). Evidence from comparative morphology and development suggest that nereidid annelids like *P. dumerilii* possess a body plan that is likely ancestral for Bilateria (Dohrn 1875; Arendt and Nübler-Jung 1994, 1997; Tessmar-Raible and Arendt 2003). This, together with its phylogenetic position in the Lophotrochozoa, makes *Platynereis* an ideal model for understanding how developmental gene regulation might have evolved from that present in the last common ancestor of all bilaterians. Additionally, *Platynereis* is also studied to understand principles of animal development (reviewed in Fischer *et al.* 2010), the hormonal regulation of regeneration *vs.* maturation (Hauenschild 1974; Hofmann 1976), and chronobiology (Hauenschild 1960; Zantke *et al.* 2013).

Descriptive studies have contributed significantly to the understanding *Platynereis* biology. These have been facilitated by reliable techniques such as *in situ* hybridization (Tessmar-Raible *et al.* 2005), quantitative PCR (Dray *et al.* 2010; Zantke *et al.* 2013), and image registration (Tomer *et al.* 2010). Established techniques for transgenesis also provide the opportunity to label specific cell types (Backfisch *et al.* 2013). Transgenic reporter lines in particular facilitate in-depth analyzes of spatio-temporal regulation of gene


doi: 10.1534/genetics.113.161091
Manuscript received December 26, 2013; accepted for publication February 17, 2014; published Early Online March 20, 2014.
Available freely online through the author-supported open access option.
Supporting information is available online at http://www.genetics.org/lookup/suppl/doi:10.1534/genetics.113.161091/-/DC1.
Sequence data from this article have been deposited in GenBank under accession nos. GU322429, EU482033, EF544399, KF937790, KF937792, and KF937791.
[1]Corresponding author: E-mail: stephanie.bannister@univie.ac.at; florian.raible@mfpl.ac.at; kristin.tessmar@mfpl.ac.at
[2]Present address: Helmholtz Zentrum München Institute of Molecular Immunology, Marchioninistr.25, 81377 Munich, Germany.

expression across the entire life cycle. This approach has already contributed to the discovery of *r-opsin1*+ peripheral photoreceptor cells (Backfisch *et al.* 2013). Coupling transgenesis with chemical-mediated cell ablation can be further used to identify the functional importance of specific cells that express a gene of interest (Veedin Rajan *et al.* 2013). While highly useful, this approach can unravel only the function of the ablated cell types, although the function of a specific gene of interest, and the protein(s) that it encodes, may well deviate from this. In addition, generating cell-type-specific transgenic lines is not trivial, considering that only few specific enhancers have been characterized for *Platynereis*.

Analysis of protein functions is also possible using methods that include the incubation of *Platynereis* larvae with small neuropeptides for studying phenotypic or behavioral phenotypes (Conzelmann *et al.* 2011), and treatment with small-molecule activators and inhibitors, to directly modulate protein functions *in vitro* (estrogen receptor) (Keay and Thornton 2009) and *in vivo* (Denes *et al.* 2007; Schneider and Bowerman 2007; Dray *et al.* 2010; Demilly *et al.* 2013; Lidke *et al.* 2014). While useful for gaining spatio-temporal insight into protein activity, the penetration (*i.e.*, effective dosage), affinity, and specificity of small-molecule inhibitors (often developed for use in other systems) may limit the pathways and targets that can be investigated *in vivo* in *Platynereis*.

Currently, the only technique available to interfere with the function of any given gene of interest in *Platynereis* is injection of morpholino antisense oligonucleotides into early stage embryos (Conzelmann *et al.* 2013). Morpholinos mediate efficient knockdown of target gene expression *in vivo* and are particularly useful for analyzing genetic phenotypes during embryogenesis and early larval development (Nasevicius and Ekker 2000). However, due to their transient action and difficulties regarding delivery into adult tissues, morpholinos are not suitable for analyzing gene function at later stages of the life cycle. Hence, to enable functional genetics studies across the entire life cycle of *Platynereis*, new tools for engineering stable and heritable gene knockouts are needed.

Transcriptional activator-like effector nucleases (TALENs) have rapidly become a technique of choice for precision genome engineering. TALENs are custom-designed nucleases that consist of a modular DNA-binding domain fused to a monomeric, C-terminal FokI nuclease domain (Christian *et al.* 2010). TALENs work in pairs and are designed to recognize and bind to tandem-oriented sequences in genomic DNA, separated by a short spacer (15–30 bp). TALEN binding causes dimerization and activation of the FokI nuclease domains, which results in cleavage of the DNA within the spacer region. Small insertions or deletions (indels) are frequently introduced at this site, as the result of errors made during DNA repair by nonhomologous end-joining (NHEJ). These indels can be up to several hundred base pairs in length and result in frameshift mutations that lead to the production of truncated or nonfunctional proteins (Sander *et al.* 2011; Lei *et al.* 2012; Ansai *et al.* 2013).

Successful use of TALENs for inducing targeted mutations has been reported in many conventional models, for example: mice (Davies *et al.* 2013; Qiu *et al.* 2013; Wang *et al.* 2013), teleost fish [zebrafish (*Danio rerio*)] (Huang *et al.* 2011; Bedell *et al.* 2012; Zu *et al.* 2013), medaka (*Oryzias latipes*) (Ansai *et al.* 2013, 2014), *Xenopus* (Ishibashi *et al.* 2012; Lei *et al.* 2012; Suzuki *et al.* 2013), and *D. melanogaster* (Liu *et al.* 2012). TALENs are also reported to be functional in a variety of other invertebrate arthropods, including mosquitos (*Aedes aegypti*) (Aryan *et al.* 2013) and *Anopheles gambiae* (Smidler *et al.* 2013), silkworm (*Bombyx mori*) (Ma *et al.* 2012; Sajwan *et al.* 2013; Takasu *et al.* 2013), and cricket (*Gryllus bimaculatus*) (Watanabe *et al.* 2012). The efficacy of TALENs across a wide variety of species, together with the availability of open-source target prediction tools, construction protocols, and reagents (available via Addgene: http://www.addgene.org/TALEN/), make this technology ideally suited for precision genome engineering in nonconventional model organisms. We therefore reasoned that TALEN technology could be used for genetic manipulation in *P. dumerilii*.

Here we report the establishment of *P. dumerilii* strains carrying TALEN-induced targeted mutations. We outline the workflow for TALEN design, construction, and *in vitro* validation and describe methods to facilitate rapid *in vivo* mutation screening of *Platynereis* larvae and adult worms, all of which can easily be adapted to other nonconventional model species. Using this workflow, we detected a variety of TALEN-induced mutations in three endogenous *Platynereis* genes. Mutation efficiencies were variable in animals raised from TALEN-injected zygotes, including evidence of biallelic mutation rates. Detection of TALEN-induced mutations in $G_1$ offspring demonstrated that such mutations are heritable. The use of TALEN-mediated genome modification provides a new opportunity to move from inferring gene functions from gene expression profiles to assigning genetic causality to biological phenotypes.

## Materials and Methods

### *Animal culture, breeding, and sampling procedures*

*Platynereis* cultures were maintained at 18° according to standard protocols as described previously (Hauenschild and Fischer 1969). Animals used for genotyping and TALEN injection were from either PIN or VIO inbred strains (as described in Zantke *et al.* 2014).

Injected larvae (G0, *i.e.*, raised from TALEN-injected zygotes, two- or four-cell-stage embryos) were sampled for mutation screening at 24 hr post fertilization (hpf) in pools of four to five individuals or as single larvae. G0 adult worms (raised from TALEN-injected embryos and sibling controls) were sampled at 1–3 months of age for genomic DNA (gDNA) extraction. Worms were anesthetized for at least 5 min in a

1:1 mixture of artificial sea water (ASW):7.5% magnesium chloride (hexahydrate, AppliChem), and a small piece of the tail (~10 segments) was removed into gDNA lysis buffer (see below for extraction). After sampling, the animals were placed into individual wells of eight-well plastic boxes containing fresh ASW and grown to maturity under standard conditions. For G1 sampling, at least 20 individual larvae (in pools of four) were screened from each batch, and remaining offspring were set out into culture boxes to be raised.

#### Genomic DNA extraction from adult worm samples

Genomic DNA was extracted from whole mature, spawned worms or tail samples from adult worms using the NucleoSpin Tissue kit (#740952, Machery-Nagel). The protocol for extraction from human or animal tissue and cultured cells was followed as described except that tail samples were extracted using half-volumes of buffers T1, proteinase K, buffer B3, and 100% ethanol, and DNA was finally eluted using 40 μl of elution buffer (gDNA from whole mature worms was eluted in 100 μl of elution buffer). Samples were stored at −20°.

#### Platynereis genes and genomic sequences used in this study

Coding sequences were previously identified for *l-cry* (GU322429: Zantke *et al.* 2013), *vtn* (EF544399: Tessmar-Raible *et al.* 2007), and *er* (EU482033: Keay and Thornton 2009). These sequences were used for designing primers for genotyping and screening PCR. Reference sequences for *er*, *l-cry*, and *vtn* genomic loci were obtained from assembly of shotgun sequence reads from BAC clones identified to include the coding sequences of each gene (*lcry*: CH305_21G18; *er*: CH305_148E21; *vtn*: CH305_55J15 and CH305_88I16). All BAC clones are available from the CHORI-305 BAC library, BAC PAC Resources, Children's Hospital Oakland Research Institute, Oakland, California. BAC screening was performed as described previously (Raible *et al.* 2005). PCR-verified genomic reference sequences for *er*, *lcry*, and *vtn* loci are available from GenBank.

#### Genotyping of Platynereis strains to identify target gene alleles

Primers were designed to amplify genomic regions for each target gene. The primer combinations used were *vtn*F1/R1, *er*F1/R1, and *l-cry*F1/R1 (see Supporting Information File S1). Genomic regions were amplified from gDNA samples prepared from 8–10 individual, mature worms from different inbred lab strains (VIO and PIN: for PCR reaction mixes see File S1). Bands corresponding to the size expected for the BAC reference allele as well as secondary bands representative of different alleles with putative size polymorphisms were subcloned. To identify single nucleotide polymorphisms (SNPs), plasmid DNA for multiple clones for each product was double-digested with *Bgl*II to excise the cloned insert, and with *Hinf*I, a frequent cutter, to generate a restriction fragment profile for each clone. Subclones representative of different restriction fragment profiles were sequenced, and sequences were compared to the BAC reference sequence to map the position and identity of the SNPs present.

#### TALEN design and construction

All TALENs were designed using the TALEN Targeter prediction tool (TAL Effector nucleotide targeter v1.0 and 2.0; https://tale-nt.cac.cornell.edu/) (Doyle *et al.* 2012). Exon sequences were used as input. The design criteria applied were the following: equal length of left and right recognition sites [*i.e.*, equal repeat variable diresidue (RVD) lengths], spacer length of 15–20 bp, NN for G recognition, and the presence of a unique restriction enzyme site in the spacer. To minimize the chance of translational bias between left and right TALENs, we aimed to standardize the size of TALEN recognition sites to 15 bp each (*i.e.*, 14.5 RVDs). TALENs (Table S1) were constructed with the GoldenGate plasmid kit (v1.0, v2.0 Addgene: 1000000024) using the reaction mixture recipes generated by inputting RVD sequences into the Golden Gate TAL Assembly form (Excel file available from https://tale-nt.cac.cornell.edu/protocols). Assembly steps were performed according to the published protocol (Cermak *et al.* 2011).

To enable *in vitro* validation of TALEN messenger RNA (mRNA) using the Sp6 mMESSAGE mMACHINE system, we constructed a new GoldenGate compatible expression vector with a pCS2+ backbone: pCS2+_TAL3-WT (Figure S1). The pCS2+_TAL3-WT vector features the long N287/C230 N- and C- terminal architecture and was constructed by inserting the TALEN cloning site from pTAL3 (GoldenGate TALEN Construction kit v1.0) (Cermak *et al.* 2011; see Figure S1 and File S1 for construction details). TALENs were also (re)constructed using the heterodimeric FokI expression plasmids pCS2TAL3-DD and pCS2TAL3-RR (Dahlem *et al.* 2012), obtained from Addgene (plasmids #37375 and #37376). All final TALEN expression vectors were sequence-verified using seqTAL_1-5 forward and TAL_R2 primers (Cermak *et al.* 2011).

#### Transcription/translation in vitro cleavage assay

TALEN efficacy was evaluated using an *in vitro* DNA cleavage assay [referred to here as transcription/translation (TnT) assay] similar to that previously described (Mussolino *et al.* 2011). Reactions were assembled using 40 μl of Sp6 Quick-coupled TnT reaction master mix (#L2080, Promega), 1 μg of each TALEN plasmid, 225 ng of specific target DNA, and 225 ng of nontarget DNA (*egfp*-coding sequence). Negative control reactions contained only left TALEN plasmid DNA. Reactions were incubated for 3 hr at 30°C. DNA was purified by phenol/chloroform extraction. Extracted DNA was treated with RNaseA and analyzed on 1.5% TAE agarose gels.

#### mRNA transcription

Plasmids encoding full-length TALENs were linearized by *Not*I digestion, gel-purified (Gel Extraction kit, Qiagen), and

used as templates for *in vitro* transcription using mMESSAGE mMACHINE Sp6 Kit (AM1340, Life Technologies). The majority of injections were performed using RNA that was not subject to further cleanup steps.

#### *Embryo microinjection*

Fertilized embryos were injected with TALEN mRNA at the one- to four-cell stage. Preparation of embryos for microinjection and microinjection techniques were performed as described previously (Backfisch *et al.* 2013). Injection solutions were prepared in a final volume of 10 μl, with 1 μl of 3% tetramethylrhodamine isothiocyanate (TRITC)–dextrane in 0.2 M KCl (Invitrogen) and equal concentrations of each TALEN mRNA (between 40 ng/μl/TALEN and 300 ng/μl/TALEN). Injection solutions were filtered using 0.45 μm PVDF centrifugal filters (Ultrafree-MC-HV, Millipore) and centrifugation at 12,000 × *g* for 1–3 min. Average injection volumes were estimated to range from 25 to 60 pl per embryo.

#### *Rapid digestion of single or pooled larvae for mutation screening*

Individual or pools of larvae ($n$ = 4–5) were harvested at, or after, 24 hpf and digested in Proteinase K/1× PCR digestion buffer (10× Qiagen PCR buffer with 1 μl Proteinase K solution per 10 μl of solution) (NucleoSpin Tissue, Machery-Nagel) at 56° for 2–3 hr. The reaction was terminated by incubation at 95° for 10 min, and samples were stored either at 4° or −20° or used directly as PCR template (1–2 μl/reaction).

#### *PCR and restriction digest screening assays*

PCR reaction mixes contained DNA polymerase [either HotStar Taq Plus (Qiagen) or Phusion Polymerase (Fermentas)], 1.5–3 mM $MgCl_2$, 400 μM dNTPs, 200 μM of each primer, 1× reaction buffer (according to the enzyme used), 1–2 μl of DNA template in final volume of 25 or 50 μl. Cycling conditions included an initial hot start at 95°–98° for 30 sec to 2 min, 35–40 cycles of 95°–98°/30 sec; 60°–68°/1 min; 72°/1–2.5 min, plus a final 72° extension for 5–10 min.

Unless otherwise stated, restriction enzymes were from New England Biolabs. In general, restriction digest reactions to screen for mutations, were incubated for 1–3 hr at 37° and heat-inactivated if necessary according to the manufacturer's instructions. See Table S2 for primer and enzyme combinations used for individual screening assays.

#### *Calculation of mutation rates using relative band intensity analysis*

We defined mutation frequency as "the percentage of samples showing evidence of TALEN-induced mutations" (as uncut PCR products from restriction digest or with extra bands representing larger insertions or deletions). We defined the mutation rate as "the percentage of mutant genome copies per sample." These values were inferred from the percentage of the total PCR product represented by mutant bands (*i.e.*, uncut PCR bands or extra insertion/deletion bands).

The relative percentages of mutant bands were calculated from gel images (TIFF format) using gel analysis tools in ImageJ (Schneider *et al.* 2012: http://rsbweb.nih.gov/ij/). The intensity of each band per lane was measured, and intensities were normalized to band size by dividing the band intensity value by the size of the band. The intensities of all bands per lane were summed to give an intensity value for the total PCR product from which the percentage of uncut, or deletion band, was calculated: *i.e.*, [$i$(uncut band)/$i$(total)] × 100 = % uncut band. These values are reported in Table 1, Table 2, and Figure S5.

## Results

To assess whether TALENs generate potential loss-of-function mutations in *P. dumerilii*, we chose to target three previously described endogenous genes: ***l**ight-receptive **cry**ptochrome* (*l-cry*), a putative circadian light receptor (Zantke *et al.* 2013); ***e**strogen **r**eceptor* (*er*), a verified ortholog of vertebrate ligand-dependent estrogen receptors (Keay and Thornton 2009); and ***v**aso**t**ocin-**n**europhysin* (*vtn*), an ortholog of oxytocin/vasopressin-neurophysin prepro-hormones (Tessmar-Raible *et al.* 2007).

#### *Genotyping to identify appropriate TALEN target sites in endogenous Platynereis genes*

TALEN efficiency is highly dependent upon specific recognition of target sequences (Cade *et al.* 2012). Hence, it is important to ensure the fidelity of reference sequences used for TALEN design and avoid targeting regions that contain polymorphisms. Genome sequencing analyses of marine invertebrates such as *Capitella teleta*, *Lottia gigantea*, sea urchin (*Strongylocentrus purpuratus*), and sponge (*Amphimedon queenslandica*) report high rates of polymorphisms (~3–5%) (Sodergren *et al.* 2006; Srivastava *et al.* 2010; Simakov *et al.* 2013b). We and others have also identified frequent SNPs present in both intronic and coding sequences of various genes in *Platynereis* laboratory strains (Simakov *et al.* 2013a; C. Lohs and F. Raible, unpublished results). Therefore, to design effective TALENs against endogenous genes, we first needed to identify the most frequent alleles present in our worm strains and determine appropriate reference sequences for TALEN design.

To identify allelic variations for *l-cry*, *er*, and *vtn*, including intron size and SNPs, each locus was analyzed by PCR-based genotyping of two related and commonly used laboratory strains of *P. dumerilii* (VIO and PIN). As frameshift mutations introduced at the 5′ end of coding sequences have a higher chance of producing truncated, nonfunctional proteins, we aimed to target the 5′ coding exons of each gene. PCR amplicons for genotyping were restricted to the first three exons of each gene, and 8–10 individuals were screened per strain. PCR products were then analyzed for size polymorphisms by restriction digest and gel electrophoresis. Clones with different restriction fragment profiles, indicative of SNPs, were sequenced, and allelic variations

**Table 1 TALEN mutation frequencies in larvae**

| Gene/TALEN pairs(s) | [TALEN mRNA][a] (ng/μl) | Total no. of screened larvae | No. of larval samples screened (*n* = no. of pooled/sample) | Mutation frequency (% mutation-positive samples) | % mutant genome copies/sample (range)[b] | % mutant genome copies/sample (average ± SD) |
|---|---|---|---|---|---|---|
| *er*Ex3_L2/_R2 | 100 | 144 | 36 (*n* = 4) | 0.0 | 0 | 0 |
| *er*Ex3_L2/_R2 | 180 | 20 | 5 (*n* = 4) | 20.0 | Not measured | NA |
| *er*Ex3_L2/_R2 | 200 | 48 | 12 (*n* = 4) | 50.0 | Not measured | NA |
| *er*Ex3_L2/_R2 | 267 | 68 | 17 (*n* = 4) | 70.6 | 2.94 - 6.08 | 4.98 ± 1.44 |
| *er*Ex3_L2/R2 | 300 | 92 | 23 (*n* = 4) | 39.1 | 5.7–13.1 | 9.02 ± 3.2 |
| *er*Ex2_L/_R + *er*Ex3_L2/_R2 | 300 | 44 | 11 (*n* = 4) | 18.2 (deletion) | 22.3–27.3 (large deletion) | 24.8 ± 3.5 (large deletion) |
| *l-cry*Ex2_L/_R + *l-cry*Ex3_L/_R | 300 | 186 | 54 (*n* = 4 × 44; *n* = 1 × 10) | 18.5 (uncut bands); 16.7 (large deletions) | 2.21–8.84 (uncut bands); 12.7–56.2 (large deletions) | 5.33 ± 2.50 (uncut bands); 35.7 ± 18.9 (large deletions) |
| *vtn*Ex2_L/R | 40 | 18 | 18 (*n* = 1) | 5.6 | Not measured | NA |
| *vtn*Ex2_L/R | 100 | 32 | 8 (*n* = 4) | 75.0 | Not measured | NA |
| *vtn*Ex2_L/R | 200 | 44 | 11 (*n* = 4) | 27.3 | 0.9–21.8 | 7.45 ± 9.00 |

[a] Final concentration of mRNA in a 10-μl injection solution per TALEN.

[b] Calculated from intensity of uncut or deletion band for samples of pooled larvae (*n* = 4–5). See also Figure S5, A and B.

were classified by aligning cloned sequences to BAC reference sequences.

We detected an ~2.5-kb polymorphism in intron 2 of the *vtn* locus in PIN strain worms (data not shown). The majority of SNPs identified for each gene were intronic and primarily present in PIN strain subclones (Figure S2 and Table S3). Only one exonic SNP was found at the 3′ end of *er* exon 2 (Table S3). In VIO worms, the majority of sequences obtained were identical to the BAC reference sequences. Hence, we concluded that the exonic BAC reference sequences were sufficient for designing TALENs to target exons of *l-cry*, *vtn*, and *er* loci.

### *TALEN design and construction*

Potential TALEN target sites were predicted for the 5′ exons of each target gene. We selected final TALEN pairs for construction based on several criteria: (1) target sites did not overlap with known SNPs or exon–intron boundaries; (2) target sites were upstream of, or within critical protein functional domains; (3) a "T" residue preceded the first nucleotide in each TALEN-binding site; and (4) spacer regions contained a unique restriction site to facilitate mutation screening by restriction digest.

Using these criteria, we selected TALEN pairs for each gene (Table S1): one pair targeting the region encoding the mature Vasotocin peptide (yellow in Figure 1A); three pairs for *er* targeting exons 2 and 3, encoding part of the N-terminal and DNA binding domains, respectively (yellow in Figure 2A); and two pairs targeting exons 2 and 3 of *l-cry*, which encode the N-terminal half of the photolyase domain (yellow in Figure 3A).

We assembled TALENs featuring two alternative backbone architectures [either with long N- and C-terminal domains (N287/C230) and the wild-type FokI domain from the pTAL3 vector (Cermak *et al.* 2011) or with the shorter backbone architecture (N136/C63) with heterodimeric DD/RR FokI domains (Dahlem *et al.* 2012). TALENs with the latter architecture are reported to mediate better mutation efficiencies and reduced capacity for nonspecific genome cleavage (Miller *et al.* 2011; Cade *et al.* 2012; Dahlem *et al.* 2012; Ansai *et al.* 2013).

### *Validation of TALEN activity for target-specific cleavage in vitro*

To test whether the TALENs were able to recognize and cleave the specific target sequence, we performed an *in vitro* cleavage assay (TnT assay), whereby TALEN expression plasmids were incubated with target DNA and nontarget DNA in a transcription translation reaction mixture. TALEN activity was assessed by the ratio of cut *vs.* uncut target DNA present following incubation. Irrespective of the assembly method, all TALEN pairs tested were found to cleave the specific target DNA with efficiencies ranging from 40 to 97% (Figure S3). Nontarget DNA was not cleaved, consistent with the observation that TALEN activity is specific for the intended target. We further compared the activity of TALENs constructed using the alternative N- and C-terminal architectures N287/C230 and N136/C63. The same TALEN pairs targeting *vtn* (*vtn*Ex2_L/R) and *er* (*er*Ex3_L1/R1) with

**Table 2 Mutation frequencies in adult worms and germline carriers in adult worms**

| Gene/TALEN pair(s) | No. of worms raised | No. of mature adults screened | No. of mutation-positive adults | Mutation frequency (% mutation-positive adults) | % mutant genome copies[a] | No. of germline carriers (carrier ID) |
|---|---|---|---|---|---|---|
| *er*Ex2_L/R + erEx3_L2/R2 | 60 | 60 | 6 | 5% (3/60 indels); 3% (2/60: large deletion); 1% (1/60: inversion) | 10–23% (indels) 6–12% (large deletions) <1% (inversion) | 2 (*er+32*; *er+59*: large deletions) |
| *er*Ex3_L2/R2 | 6 | 6 | 0 | 0% | NA | NA |
| *l-cry*Ex2_L/R + *l-cry*Ex3_L/R | >80 | 62 | 27 | 43% (27/60: indels) 9% (6/60: large deletions and indels) | 5–~100% (indels) Not measured | 1 (*l-cry+36*: indels and large deletion) |
| *vtn*Ex2_L/R | 13 | 13 | 3 | 20% (indels) | Not measured | 0 |

Calculated from intensity of uncut or deletion band. Indicates individual mutation rate. See also Figure S5C.

the shorter N136/C63 architecture were more efficient by 30 and 7%, respectively, compared to those with the longer N287/C230 architecture (Figure S3D). Based on these findings, we proceeded to validate the activity of TALENs made using the N136/C63 architecture *in vivo*.

### *Validation of TALEN activity and efficiency in vivo*

To test whether the constructed TALENs were active *in vivo*, embryos were injected with various concentrations of mRNA encoding either a single TALEN pair per gene (*vtn* and *er*) or two TALEN pairs targeting different exons of the same gene (*er* and *l-cry*). To screen for TALEN-induced indel mutations in the endogenous target genes, we established a method for digesting single or small pools of larvae and using this lysate as template for PCR (see *Materials and Methods*). This facilitated mutation screening of TALEN-injected animals (injected at zygote/two- or four-cell stage) at larval stages of development (as early as 24 hpf), thereby enabling rapid validation of TALEN efficacy and activity *in vivo*.

If mutations are induced that disrupt the restriction site, the PCR product should be either completely or partially resistant to digestion. PCR without digestion was also used to screen for larger indel mutations and long-range deletions resulting from simultaneous cleavage by two TALEN pairs.

### *Predicted loss-of-function mutations detected in TALEN-injected larvae and adult worms*

Evidence of mutations in TALEN-injected larvae was detected for all three genes (Figure 1, Figure 2, Figure 3). Sequencing of subcloned, digest-resistant (here referred to as "uncut") PCR products revealed a variety of small deletions ranging in size from 1 to 23 bp and insertions of 1–19 bp (Figure 1, B and D; Figure 2, B and F; Figure 3, B and C). In one case, we detected a 109-bp insertion at the *vtn* target site (Figure 1, red arrow in B and green sequence in D). Blastn analysis revealed exact homology of this inserted sequence with part of intron 3 of the *vtn* locus (Figure 1A).

Subsequently, adult worms were raised from embryos injected with TALENs against each of the three target genes. Sequencing of uncut PCR products from these worms recovered similar indel mutations as those detected in larval samples (Figure 1, C and D; Figure 2, C–F; Figure 3, C–E).

Of the mutant sequences obtained, ~70% represented frameshift mutations resulting in premature stop codons. These results validate that TALENs induce targeted, predicted loss-of-function mutations in endogenous genomic loci *in vivo*.

### *Simultaneous cleavage by two TALEN pairs induces long-range deletions*

Simultaneous cleavage by two TALEN pairs targeting different sites of the same locus or chromosome was shown to induce long-range deletions in different species (Gupta *et al.* 2013). We therefore investigated whether co-injection of two TALEN pairs targeting different exons of the same gene induce large genomic deletions in *Platynereis*. We screened for deletions using PCR assays that amplify a region of the locus

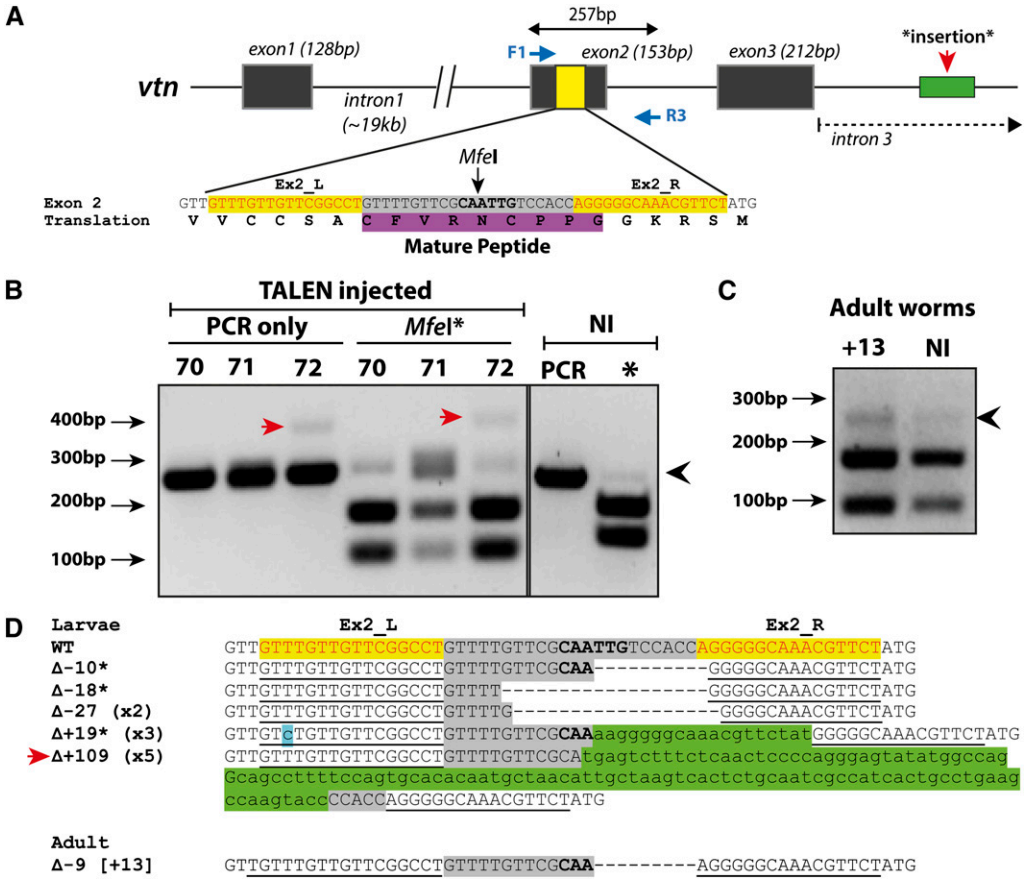


**Figure 1** Evidence for TALEN-induced mutation of *Platynereis vasotocin-neurophysin*. (A) Schematic of the *vtn* locus showing TALEN target site (yellow) in exon 2 (L, left TALEN; R, right TALEN). Blue arrows (F1/R3) indicate primers used for mutation screening PCR [size of amplicon (bp) indicated by double-ended arrows]. Green block indicates position of sequence from intron 3 detected as an insertion (sample 72). The mature peptide (highlighted in purple) is included by the majority of the TALEN spacer and includes the *Mfe*I-screening site. (B) Restriction digest screening of 24-hpf larvae injected with *vtn*Ex2_L and *vtn*Ex2_R TALEN mRNA at concentration of 200 ng/μl/TALEN. Samples contain pools of four larvae. Black arrow indicates size of uncut PCR product; red arrow indicates 109-bp insertion detected in sample 72. (C) Results of *Mfe*I digest of PCR products from adult worms: uncut PCR product (black arrowhead) cloned from adult injected worm *vtn+13*, representing 9-bp deletion. (B and C) PCR, un-digested PCR product; NI, non-injected; asterisk (*) indicates samples digested with *Mfe*I. (D) Results of sequence analysis of uncut and insertion bands from samples in B and C. Length of mutations indicated by Δ symbol with "−" indicating deletions and "+" indicating insertions. Restriction site is shown in boldface type; asterisks indicate frameshift mutations. Shading key: yellow, TALEN-binding sites; gray, spacer; blue, nucleotides differing from wild type; green, inserted nucleotides.

containing both TALEN recognition sites in the *er* and *l-cry* genes, respectively (Figure 2A and Figure 3A).

In addition to wild-type PCR products, smaller bands corresponding to the size expected for long-range deletions were detected in animals co-injected with TALENs targeting different exons of *er* and *l-cry* (Figure 2, E and F; Figure 3, B and C). Sequencing of subcloned small bands confirmed the presence of deletions with breakpoints that correspond to the spacer regions of the two respective TALEN target sites.

At the *er* locus, deletions of 1568 and 1575 bp were recovered in both larvae and individual adult worms (Figure 2E, red arrows; Figure 2F, bottom). These deletions remove the majority of the DNA-binding domain. In addition, we detected one inversion event at the *er* locus (*er*+7: 1/60 animals, Figure S4). At the *l-cry* locus, a 409-bp long-range deletion was sequence-confirmed, which resulted in a frameshift and thus a premature stop codon (Figure 3B, red arrow; Figure 3C). Together, these results show that co-injection of two TALEN pairs targeting the same locus can induce long-range deletions in *P. dumerilii*.

### *Individual mutation rates in TALEN-injected worms*

To estimate the efficiency of individual TALEN pairs, or TALEN pair combinations, we analyzed mutation frequencies as the percentage of larval samples or individual worms for which evidence of mutant PCR products could be detected. Uncut PCR products representative of indel mutations were detected in 5–75% of TALEN-injected larval samples (Table 1) and in 5–43% of adult TALEN-injected worms (Table 2). Long-range deletions resulting from cleavage with two TALEN pairs were detected in larval samples at frequencies of 16–18% (Table 1) and in 3–9% of individual adult worms (Table 2).

To estimate the percentage of the genome modified in individual animals or larval samples (*i.e.*, mutation rate), we calculated the percentage of mutant PCR products (uncut, or short deletion bands) relative to the total PCR product. TALEN efficiencies in pooled larvae ranged between ~1 and 21% and between 6 and 52% in adult worms (Table 1; Table 2; Figure S5). The highest efficiency was detected for the *l-cry* exon 3 TALENs, with completely uncut PCR products representing likely biallelic mutations detected in 2 of 62 injected worms (Figure 3D: *l-cry+45*, Table 2). The high frequency of TALEN-induced mutations detectable in individual worms, combined with individual mutation rates of up to 100%, demonstrate that TALENs are highly efficient tools for engineering targeted mutations in endogenous *Platynereis* genes.

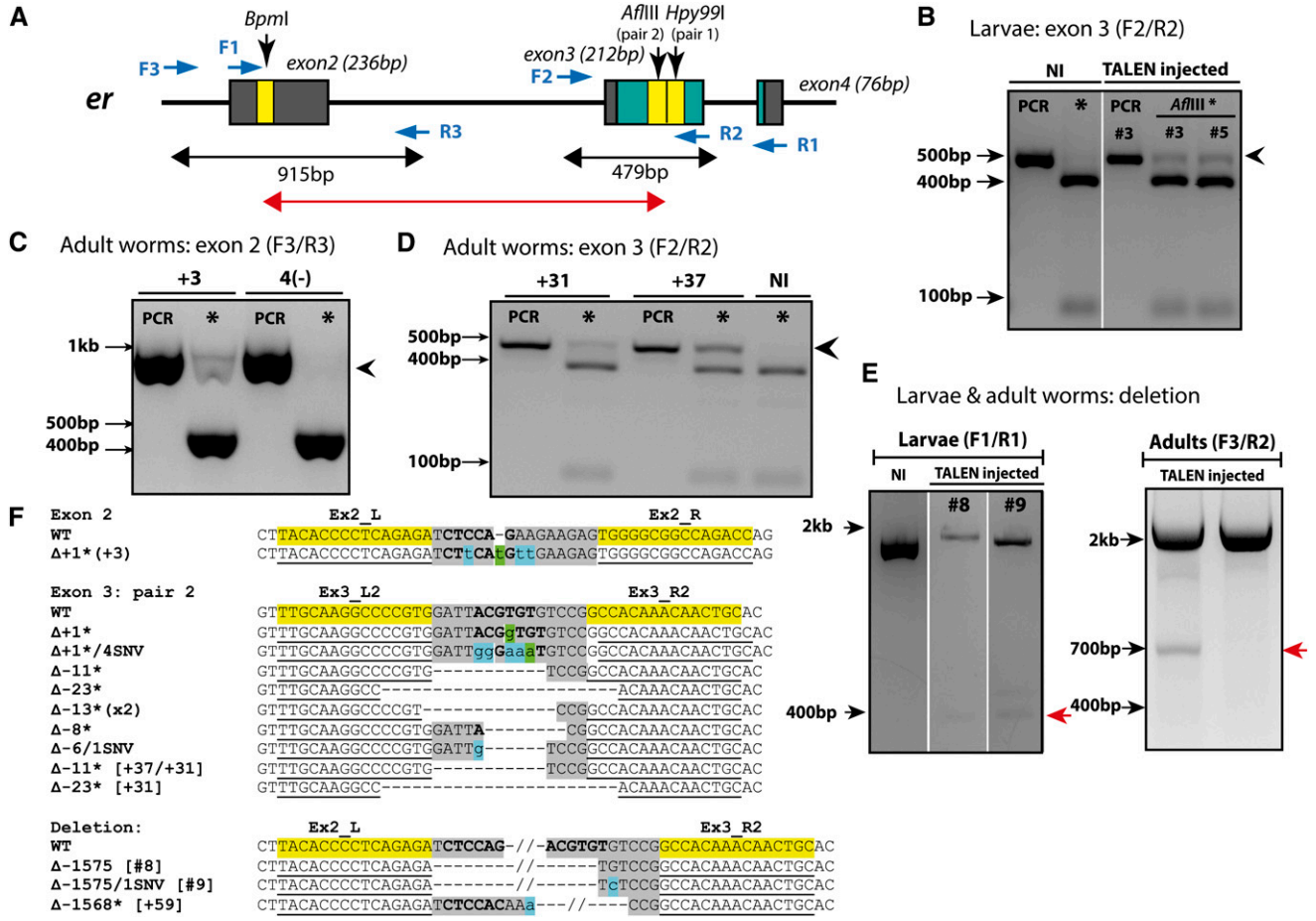


**Figure 2** TALEN-induced mutations in the *Platynereis estrogen receptor*. (A) Schematic of the *er* locus showing target exons 2 and 3 with TALEN target sites (yellow). Blue arrows, primer positions; red double-ended arrow, region of sequence deleted in E; green, DNA-binding domain. Primer combinations used for screening are shown above in B–E. (B–E) PCR, undigested PCR product; NI, non-injected. (B) Restriction digest screening of larvae injected with *er*Ex3_L2/R2 TALENs (mRNA concentration: 267 ng/μl/TALEN mRNA). Arrowhead indicates uncut PCR product following *Afl*II digestion (asterisk). (C) Mutation evidence at exon 2 site: uncut band adult worm +3 *vs.* fully digested product from mutation-negative (−) TALEN-injected worm. (D) Adult worms *er+31* and *er+37* with mutations at exon 3 site. (E) Deletions (red arrow) detected in larvae and adult worms resulting from simultaneous cleavage at exons 2 and 3 using 300 ng/μl/TALEN mRNA: deletion positive (+); deletion negative (−). Please note different primer pairs used for larval *vs.* adult samples. (F) Mutant sequences obtained from digest screening for exons 1, 2, and long deletions. Numbers in brackets indicate the sample or worm from which the sequence was obtained; all other sequences are from injected larvae shown in B. Length of mutations are indicated by Δ with "−" indicating deletions and "+" indicating insertions. Restriction site is shown in boldface type; asterisks indicate frameshift mutations. Shading key: yellow, TALEN binding sites; gray, spacer; blue, nucleotides differing from wild type; green, inserted nucleotides.

### *Germline transmission of TALEN-induced mutations*

In a variety of animal models, TALEN-induced mutations have been shown to occur in the germline, thus facilitating the establishment of mutant lines (Cade *et al.* 2012; Aryan *et al.* 2013; Qiu *et al.* 2013; Sajwan *et al.* 2013). To validate that TALENs can also mediate germline mutations in *Platynereis*, we analyzed the offspring of mutation-positive adult worms for evidence of transmitted mutations. We screened small pools of G1 larvae from mutation-positive mature worms. Germline transmission rates were estimated based on the number of heterozygous mutant G1 larvae detected.

We identified three germline mutation carriers (Table 2): one transmitting both long-range deletions and frameshift mutations at the *l-cry* exon 3 site (*l-cry+36*: Figure 4, A and B) and two transmitting long-range deletions of the *er* locus (*er +32* and *er+59*: Figure 4, C and D).

Mutations were detected in ~3% of the G1 screened from *er* carriers and 40% of the G1 screened from the *l-cry* carrier (Table 2). Sequencing revealed that the same mutations were present in the G1 and the respective parent. These results demonstrate that TALEN-induced mutations are both stable and heritable in *Platynereis*.

### *Survival rates of TALEN-injected worms*

To assess the possible impact of the TALEN injection procedure on the normal development of *Platynereis* embryos, we analyzed larval survival data. In general, rates of normal development were highly variable among different batches (Figure S6A), a phenomenon frequently observed when crossing animals to maintain the laboratory culture. Neither higher concentrations of TALEN mRNA nor co-injection of two TALEN pairs *vs.* a single pair appeared to have a

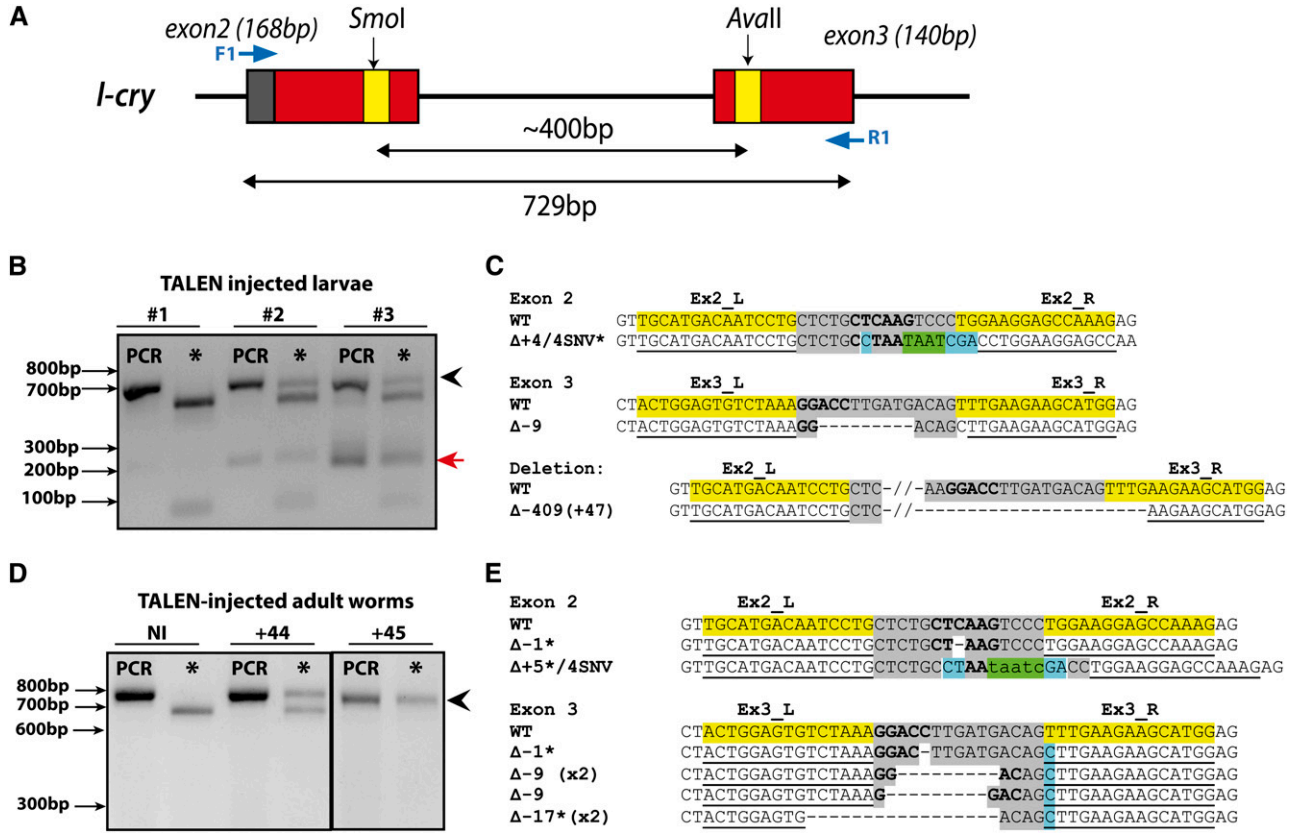


**Figure 3** Evidence of TALEN-induced mutations at *l-cry* locus. (A) Schematic of the *l-cry* genomic locus. Gray, exons; red, photolyase domain; yellow, TALEN sites; blue arrows, position of primers. Size of PCR amplicons and distance between TALEN sites indicated by double-ended arrows. Mutation screening results from larvae (B) and adult worms (D) injected with TALENn mRNA (*l-cry*Ex2_L/R and *l-cry*Ex3_L/R: 300 ng/μl/TALEN), showing uncut PCR bands following *Ava*II digestion (black arrow) and/or long deletions (red arrow). (D) Worm *l-cry+45* shows completely undigested band suggesting biallelic mutation. Mutant sequences obtained from injected larvae (C) and adult worms (E) following *Ava*II digestion (asterisks). Length of mutations indicated by Δ with "−" indicating deletions and "+" indicating insertions. Restriction site is shown in boldface type; asterisks indicate frameshift mutations. Shading key: yellow, TALEN0binding sites; gray, spacer; blue, nucleotides differing from wild type; green, inserted nucleotides. (B and D) PCR, undigested PCR product; NI, non-injected.

negative impact upon survival at 24 hpf (Figure S6A and Table S4). This is evidenced by the fact that we did not observe any obvious differences in the proportions of normal *vs.* mis-developed embryos in TRITC+ *vs.* TRITC− embryos (Figure S6B).

Of the embryos injected and set out to be raised, between 77 and 100% survived to adulthood (Table S4). Spawning data were also recorded for *vtn* and *er* TALEN-injected worms. The majority of worms spawned during new moon phases (Figure S7), in line with normal spawning rhythms observed under our laboratory conditions (Zantke *et al.* 2013). These collective observations suggest that delivery of TALEN mRNA into *Platynereis* is generally nontoxic.

Taken together with the results of the mutation analyses and germline transmission evidence, we conclude that TALENs represent a highly suitable approach for generating stable and heritable genomic modifications in *P. dumerilii*.

## Discussion

We have adapted TALENs to engineer heritable, predicted loss-of-function mutations in three endogenous genes of the marine annelid *P. dumerilii*. Detectable mutations included short indels that localize to spacer regions of TALEN recognition sites, as well as long-range deletions when co-injecting two TALEN pairs targeting the same locus. The detection of potential biallelic mutation of *l-cry* in injected worms exemplifies that TALENs are highly efficient tools for genome modification in *Platynereis* that can be used to establish genetic mutant lines.

### *TALENs cause a variety of mutation types at variable frequencies in Platynereis*

Injection of TALEN mRNA into *Platynereis* zygotes induced a range of mutations at target sites. Indel mutations varied in size from 1 to 110 bp while long-range deletions of up to 1.5 kb were generated by co-injection of two TALEN pairs. This variety of mutations is similar to what has been shown for TALEN-mediated *in vivo* genome modification studies in other model systems (Ma *et al.* 2012; Qiu *et al.* 2013; Xiao *et al.* 2013). The use of PCR and restriction digest screening, as we demonstrate here, is both rapid and effective for detecting mutations. However, this approach may not detect mutations at single TALEN sites where the restriction site is

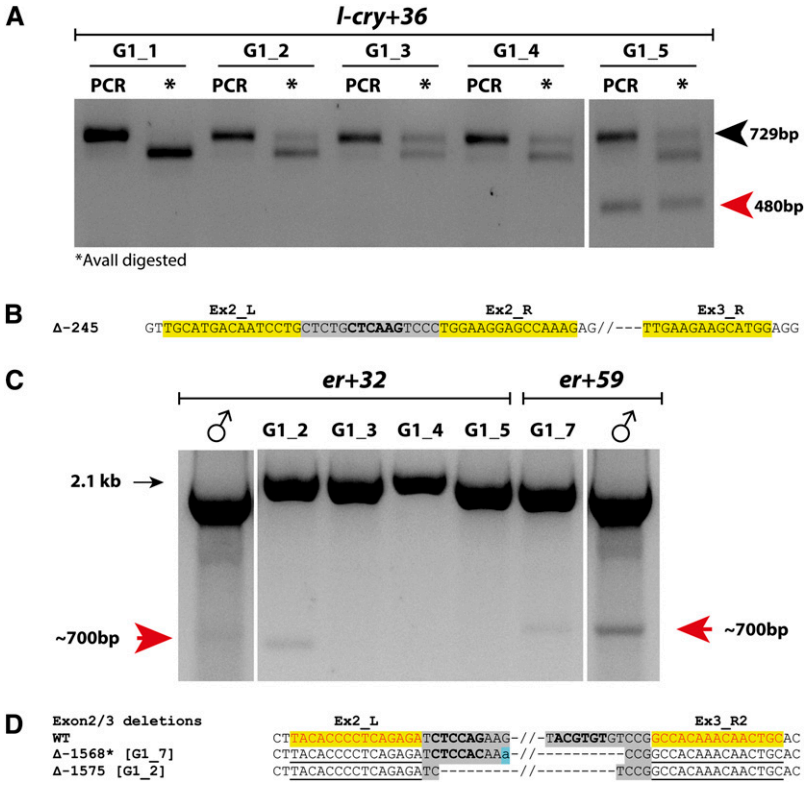


**Figure 4** Evidence for germline transmission of TALEN-mediated mutations. (A) Mutation screening results: G1 from male worm (*l-cry+36*) injected with *l-cry* TALENs. Pools of four G1 larvae were digested using proteinase K buffer and analyzed by PCR and *Ava*II digestion. Aliquots of undigested PCR products (PCR) are run next to a digested aliquot (*) for each sample. Sample G1_5 shows both uncut (black arrowhead) and deletion (red arrowhead) bands. (B) Sequence of uncut band in sample G1_5 in A. (C and D) Evidence of long-range deletions (red arrows) in pooled G1 larvae from *er* TALEN-injected worms *er+32* and *er+59* (male symbols indicate PCR products from these male worms). (D) Sequenced deletions from G1 samples: G1_2 and G1_7 shown in C. Asterisks indicate frameshift mutations.

not disrupted; hence, our results may under-represent the actual mutation rates present in individual animals.

Compared with long-range deletions, inversion events are rare and have only been reported *in vivo* at rates of 0.2–1% and 4% in zebrafish (Gupta *et al.* 2013; Xiao *et al.* 2013) and pigs (Carlson *et al.* 2012), respectively. In agreement with this, we detected long-range deletions in a number of animals at mutation rates of up to 9%, while only one inversion event was observed in a single animal, for which the rate is likely <1% (Figure S4).

Our collective data show that TALEN efficiencies are highly variable in *Platynereis*. We could detect mutations in 3–43% of adult TALEN-injected worms, and mutation rates detected in individual worms ranged from 6% up to potential biallelic (~100%) modification. Mutation rates calculated for individual worms were also variable, both between different individuals injected with the same TALENs and between the different TALEN pairs tested (Figure S5). Why different TALEN pairs elicit such variable mutation efficiencies *in vivo* is generally not well understood. Factors that likely relate to the sequence of the TALENs themselves or accessibility of the target sites could explain at least part of the observed variation.

Interestingly, a large insertion that we detected at the *vtn* TALEN site was found to be exactly homologous to part of intron 3. Gene insertion can occur following TALEN-induced cleavage, via homologous recombination, or NHEJ mechanisms (reviewed in Gaj *et al.* 2013 and Joung and Sander 2013). We noted that a 3-bp GCA motif was shared between the 5′ end of this insertion and the 5′ breakpoint in the TALEN spacer. Aside from this, however, we could not find any contiguous sequence homology between intron 3 in the region flanking the inserted sequence and the TALEN target site. While this 3-bp homology might argue for NEHJ-mediated insertion, we cannot explain exactly how or why this particular sequence was inserted. Regardless of the underlying mechanism, however, this integration event already provides evidence that TALEN-induced cleavage can mediate insertion of alternative sequences at TALEN sites *in vivo*.

### *Workflow and recommendations for TALEN use in emerging molecular model organisms*

In the process of establishing TALENs as tools for genome modification in *Platynereis*, we streamlined several protocols together into a single workflow (for a summarizing workflow scheme, see also Zantke *et al.* 2014). Our workflow encompasses everything from screening for allelic variation at the target genomic locus to TALEN design and construction, *in vitro* validation, and *in vivo* mutation screening approaches, all of which can be applied to facilitate establishment of TALENs for genome modification in other emerging molecular model species. In addition to adapting and combining existing methods described for TALEN design (Miller *et al.* 2011), construction (Cermak *et al.* 2011), *in vitro* validation, and mutation screening via restriction digestion (Mussolino *et al.* 2011), we included two additional steps: (1) establishing quality reference sequences through initial genotyping and analysis of allelic frequencies and (2) developing methods to screen for *in vivo* TALEN activity in small pools of larvae shortly after injection.

The initial genotyping to identify SNPs and validate appropriate genomic reference sequences was crucial for TALEN design. TALEN efficiency *in vivo* is reported to be significantly decreased where mismatches are present in one or both of the TALEN recognition sequences (Cade *et al.* 2012; Dahlem *et al.* 2012). Thus, for emerging model systems with possible high rates of polymorphisms we recommend to first genotype and define appropriate reference genomic sequences for the target strain to maximize potential TALEN efficiencies.

The second adaptation of our workflow was the optimization of a protocol to prepare crude gDNA templates from small pools of larvae. This was crucial for rapid validation of TALEN activity *in vivo* by PCR. By generating crude gDNA lysates from injected larvae, we could analyze different batches of injected animals separately, rather than pool animals together from several injections, which would have been required for gDNA extraction using kit-based methods. This enabled both a rapid assessment of TALEN activity *in vivo* and a more accurate estimation of mutation frequencies. In other species, phenotype scoring has been used to demonstrate proof of TALEN activity *in vivo* (Dahlem *et al.* 2012; Liu *et al.* 2012; Ma *et al.* 2012; Aryan *et al.* 2013; Suzuki *et al.* 2013; Wang *et al.* 2013). However, this is difficult to apply when evaluating TALEN efficiency for genes with unpredictable phenotypes and may be impractical for rapidly assessing TALEN functionality *in vivo* against genes where phenotypes are not observable until adult stages of the life cycle.

The genotyping and rapid larval digestion protocols that we introduced here can also be equally applied to other genome-editing systems, such as the recently described Cas9/CRISPR system (Cong *et al.* 2013; Mali *et al.* 2013). Cas9/CRISPR technology involves the use of short guide RNAs (sgRNAs) that direct a bacterially derived endonuclease (Cas9) to recognize specific sites in the genome and induce DNA double-strand breaks (Jinek *et al.* 2012). The initial version of the system caused high numbers of off-target mutations (Fu *et al.* 2013), which was improved by the simultaneous use of two sgRNAs and a mutant nickase version of the Cas9 protein (Ran *et al.* 2013) and most recently by shortening the length of the sgRNA (Fu *et al.* 2014). While the production of Cas9/CRISPR reagents is more straightforward than constructing TALENs and thus potentially useful for multiplex functional screens, possible target sites are more limited than in the case of TALENs (reviewed in Blackburn *et al.* 2013). Furthermore, as both systems use very different initial mechanisms of DNA sequence recognition, it is possible that in some cases where one system fails or is inefficient, the other might work better (Hwang *et al.* 2013; Auer *et al.* 2014). In the future, it will be useful to explore the efficiency of TALEN and Cas9/CRISPR systems in parallel to further enhance the capacity for targeted genome modification in *P. dumerilii*.

In conclusion, we have demonstrated that TALENs mediate targeted and heritable mutation of endogenous genes in the marine annelid *P. dumerilii* and provide a streamlined workflow that can serve as a template for the establishment of TALEN technology in other nonconventional and emerging model organisms.

## Acknowledgments

We thank all three anonymous reviewers for their positive comments and constructive feedback on our manuscript and Poonam Sharma, Andrij Belokurov, and Verena Hoellbacher for feeding and maintaining the *Platynereis* cultures and assistance with animal care for TALEN-injected worms. This work was supported by funds of the Max F. Perutz Laboratories (http://www.mfpl.ac.at/home.html), the research platform "Marine rhythms of Life" of the University of Vienna (to K.T.-R. and F.R.); START award (#AY0041321) from the Fond zur Förderung der wissenschaftlichen Forschung (www.fwf.ac.at); and a Human Frontier Science Program (http://www.hfsp.org/) research grant (#RGY0082/2010) (to K.T.-R.). The research leading to these results has received funding from the European Research Council under the European Community's Seventh Framework Programme (FP7/2007-2013)/ERC Grant Agreement 260304 (to F.R.) and (FP7/2007-2013)/ERC Grant Agreement 337011 (to K.T.-R.). S.B. is funded by the Max F. Perutz Laboratories Vienna International PostDoctoral Program for Molecular Life Sciences (funded by Austrian Ministry of Science and Research and City of Vienna, Cultural Department—Science and Research). The funders had no role in study design, data collection and analysis, decision to publish, or preparation of the manuscript.

*Note added in proof*: See Zantke *et al.* 2014 (pp. 19–31) in this issue for a related work.

## Literature Cited

Ansai, S., T. Sakuma, T. Yamamoto, H. Ariga, N. Uemura *et al.*, 2013 Efficient targeted mutagenesis in medaka using custom-designed transcription activator-like effector nucleases. Genetics 193: 739–749.

Ansai, S., K. Inohaya, Y. Yoshiura, M. Schartl, N. Uemura *et al.*, 2014 Design, evaluation, and screening methods for efficient targeted mutagenesis with transcription activator-like effector nucleases in medaka. Dev. Growth Differ. 56: 98–107.

Arendt, D., and K. Nübler-Jung, 1994 Inversion of dorsoventral axis? Nature 371: 26.

Arendt, D., and K. Nübler-Jung, 1997 Dorsal or ventral: similarities in fate maps and gastrulation patterns in annelids, arthropods and chordates. Mech. Dev. 61: 7–21.

Aryan, A., M. A. Anderson, K. M. Myles, and Z. N. Adelman, 2013 TALEN-based gene disruption in the dengue vector Aedes aegypti. PLoS ONE 8: e60082.

Auer, T. O., K. Duroure, A. De Cian, J. P. Concordet, and F. Del Bene, 2014 Highly efficient CRISPR/Cas9-mediated knock-in in zebrafish by homology-independent DNA repair. Genome Res. 24: 142–153.

Backfisch, B., V. B. Veedin Rajan, R. M. Fischer, C. Lohs, E. Arboleda *et al.*, 2013 Stable transgenesis in the marine annelid *Platynereis*

*dumerilii* sheds new light on photoreceptor evolution. Proc. Natl. Acad. Sci. USA 110: 193–198.

Bedell, V. M., Y. Wang, J. M. Campbell, T. L. Poshusta, C. G. Starker *et al.*, 2012 In vivo genome editing using a high-efficiency TALEN system. Nature 491: 114–118.

Blackburn, P. R., J. M. Campbell, K. J. Clark, and S. C. Ekker, 2013 The CRISPR system: keeping zebrafish gene targeting fresh. Zebrafish 10: 116–118.

Cade, L., D. Reyon, W. Y. Hwang, S. Q. Tsai, S. Patel *et al.*, 2012 Highly efficient generation of heritable zebrafish gene mutations using homo- and heterodimeric TALENs. Nucleic Acids Res. 40: 8001–8010.

Carlson, D. F., W. Tan, S. G. Lillico, D. Stverakova, C. Proudfoot *et al.*, 2012 Efficient TALEN-mediated gene knockout in livestock. Proc. Natl. Acad. Sci. USA 109: 17382–17387.

Cermak, T., E. L. Doyle, M. Christian, L. Wang, Y. Zhang *et al.*, 2011 Efficient design and assembly of custom TALEN and other TAL effector-based constructs for DNA targeting. Nucleic Acids Res. 39: e82.

Christian, M., T. Cermak, E. L. Doyle, C. Schmidt, F. Zhang *et al.*, 2010 Targeting DNA double-strand breaks with TAL effector nucleases. Genetics 186: 757–761.

Cong, L., F. A. Ran, D. Cox, S. Lin, R. Barretto *et al.*, 2013 Multiplex genome engineering using CRISPR/Cas systems. Science 339: 819–823.

Conzelmann, M., S. L. Offenburger, A. Asadulina, T. Keller, T. A. Munch *et al.*, 2011 Neuropeptides regulate swimming depth of Platynereis larvae. Proc. Natl. Acad. Sci. USA 108: E1174–E1183.

Conzelmann, M., E. A. Williams, S. Tunaru, N. Randel, R. Shahidi *et al.*, 2013 Conserved MIP receptor-ligand pair regulates *Platynereis* larval settlement. Proc. Natl. Acad. Sci. USA 110: 8224–8229.

Dahlem, T. J., K. Hoshijima, M. J. Jurynec, D. Gunther, C. G. Starker *et al.*, 2012 Simple methods for generating and detecting locus-specific mutations induced with TALENs in the zebrafish genome. PLoS Genet. 8: e1002861.

Davies, B., G. Davies, C. Preece, R. Puliyadi, D. Szumska *et al.*, 2013 Site specific mutation of the Zic2 locus by microinjection of TALEN mRNA in mouse CD1, C3H and C57BL/6J oocytes. PLoS ONE 8: e60216.

Demilly, A., P. Steinmetz, E. Gazave, L. Marchand, and M. Vervoort, 2013 Involvement of the Wnt/beta-catenin pathway in neurectoderm architecture in Platynereis dumerilii. Nat. Commun. 4: 1915.

Denes, A. S., G. Jekely, P. R. Steinmetz, F. Raible, H. Snyman *et al.*, 2007 Molecular architecture of annelid nerve cord supports common origin of nervous system centralization in bilateria. Cell 129: 277–288.

Dohrn, A., 1875 *The Origin of Vertebrates and the Principle of Functional Change* (in German). Verlag von Wilhelm Engelmann, Leipzig, Germany.

Doyle, E. L., N. J. Booher, D. S. Standage, D. F. Voytas, V. P. Brendel *et al.*, 2012 TAL Effector-Nucleotide Targeter (TALE-NT) 2.0: tools for TAL effector design and target prediction. Nucleic Acids Res. 40(Web Server issue): W117–W122.

Dray, N., K. Tessmar-Raible, M. Le Gouar, L. Vibert, F. Christodoulou *et al.*, 2010 Hedgehog signaling regulates segment formation in the annelid *Platynereis*. Science 329: 339–342.

Fischer, A. H., T. Henrich, and D. Arendt, 2010 The normal development of *Platynereis dumerilii* (Nereididae, Annelida). Front. Zool. 7: 31.

Fu, Y., J. A. Foden, C. Khayter, M. L. Maeder, D. Reyon *et al.*, 2013 High-frequency off-target mutagenesis induced by CRISPR-Cas nucleases in human cells. Nat. Biotechnol. 31: 822–826.

Fu, Y., J. D. Sander, D. Reyon, V. M. Cascio, and J. K. Joung, 2014 Improving CRISPR-Cas nuclease specificity using truncated guide RNAs. Nat. Biotechnol. 32: 279–284.

Gaj, T., C. A. Gersbach, and C. F. Barbas, III, 2013 ZFN, TALEN, and CRISPR/Cas-based methods for genome engineering. Trends Biotechnol. 31: 397–405.

Gupta, A., V. L. Hall, F. O. Kok, M. Shin, J. C. McNulty *et al.*, 2013 Targeted chromosomal deletions and inversions in zebrafish. Genome Res. 23: 1008–1017.

Hauenschild, C., 1960 Lunar periodicity. Cold Spring Harb. Symp. Quant. Biol. 25: 491–497.

Hauenschild, C., 1974 Endocrine control of sexual development in some polychaetes (in German). Fortschr. Zool. 22: 75–92.

Hauenschild, C., and A. Fischer, 1969 pp. 1–55 in *Platynereis dumerilii. Mikroskopische Anatomie, Fortpflanzung, Entwicklung* [*Platynereis dumerilii. Microscopical Anatomy, Reproduction and Development*]. Groses Zoologisches Praktikum Heft, Stuttgart, Germany.

Hofmann, D. K., 1976 Regeneration and endocrinology in the polychaete Platynereis dumerilii: an experimental and structural study. Dev. Genes Evol. 180: 47–71.

Huang, P., A. Xiao, M. Zhou, Z. Zhu, S. Lin *et al.*, 2011 Heritable gene targeting in zebrafish using customized TALENs. Nat. Biotechnol. 29: 699–700.

Hwang, W. Y., Y. Fu, D. Reyon, M. L. Maeder, S. Q. Tsai *et al.*, 2013 Efficient genome editing in zebrafish using a CRISPR-Cas system. Nat. Biotechnol. 31: 227–229.

Ishibashi, S., R. Cliffe, and E. Amaya, 2012 Highly efficient biallelic mutation rates using TALENs in Xenopus tropicalis. Biol. Open 1: 1273–1276.

Jinek, M., K. Chylinski, I. Fonfara, M. Hauer, J. A. Doudna *et al.*, 2012 A programmable dual-RNA-guided DNA endonuclease in adaptive bacterial immunity. Science 337: 816–821.

Joung, J. K., and J. D. Sander, 2013 TALENs: a widely applicable technology for targeted genome editing. Nat. Rev. Mol. Cell Biol. 14: 49–55.

Keay, J., and J. W. Thornton, 2009 Hormone-activated estrogen receptors in annelid invertebrates: implications for evolution and endocrine disruption. Endocrinology 150: 1731–1738.

Lei, Y., X. Guo, Y. Liu, Y. Cao, Y. Deng *et al.*, 2012 Efficient targeted gene disruption in Xenopus embryos using engineered transcription activator-like effector nucleases (TALENs). Proc. Natl. Acad. Sci. USA 109: 17484–17489.

Lidke, A. K., S. Bannister, A. M. Lower, D. M. Apel, M. Podleschny *et al.*, 2014 17beta-Estradiol induces supernumerary primordial germ cells in embryos of the polychaete *Platynereis dumerilii*. Gen. Comp. Endocrinol. 196: 52–61.

Liu, J., C. Li, Z. Yu, P. Huang, H. Wu *et al.*, 2012 Efficient and specific modifications of the *Drosophila* genome by means of an easy TALEN strategy. J. Genet. Genomics 39: 209–215.

Ma, S., S. Zhang, F. Wang, Y. Liu, H. Xu *et al.*, 2012 Highly efficient and specific genome editing in silkworm using custom TALENs. PLoS ONE 7: e45035.

Mali, P., L. Yang, K. M. Esvelt, J. Aach, M. Guell *et al.*, 2013 RNA-guided human genome engineering via Cas9. Science 339: 823–826.

Miller, J. C., S. Tan, G. Qiao, K. A. Barlow, J. Wang *et al.*, 2011 A TALE nuclease architecture for efficient genome editing. Nat. Biotechnol. 29: 143–148.

Mussolino, C., R. Morbitzer, F. Lutge, N. Dannemann, T. Lahaye *et al.*, 2011 A novel TALE nuclease scaffold enables high genome editing activity in combination with low toxicity. Nucleic Acids Res. 39: 9283–9293.

Nasevicius, A., and S. C. Ekker, 2000 Effective targeted gene 'knockdown' in zebrafish. Nat. Genet. 26: 216–220.

Qiu, Z., M. Liu, Z. Chen, Y. Shao, H. Pan *et al.*, 2013 High-efficiency and heritable gene targeting in mouse by transcription activator-like effector nucleases. Nucleic Acids Res. 41: e120.

Raible, F., K. Tessmar-Raible, K. Osoegawa, P. Wincker, C. Jubin *et al.*, 2005 Vertebrate-type intron-rich genes in the marine annelid Platynereis dumerilii. Science 310: 1325–1326.

Ran, F. A., P. D. Hsu, C. Y. Lin, J. S. Gootenberg, S. Konermann *et al.*, 2013 Double nicking by RNA-guided CRISPR Cas9 for enhanced genome editing specificity. Cell 154: 1380–1389.

Sajwan, S., Y. Takasu, T. Tamura, K. Uchino, H. Sezutsu *et al.*, 2013 Efficient disruption of endogenous Bombyx gene by TAL effector nucleases. Insect Biochem. Mol. Biol. 43: 17–23.

Sander, J. D., L. Cade, C. Khayter, D. Reyon, R. T. Peterson *et al.*, 2011 Targeted gene disruption in somatic zebrafish cells using engineered TALENs. Nat. Biotechnol. 29: 697–698.

Schneider, C. A., W. S. Rasband, and K. W. Eliceiri, 2012 NIH Image to ImageJ: 25 years of image analysis. Nat. Methods 9: 671–675.

Schneider, S. Q., and B. Bowerman, 2007 beta-Catenin asymmetries after all animal/vegetal-oriented cell divisions in *Platynereis dumerilii* embryos mediate binary cell-fate specification. Dev. Cell 13: 73–86.

Simakov, O., T. A. Larsson, and D. Arendt, 2013a Linking micro- and macro-evolution at the cell type level: a view from the lophotrochozoan *Platynereis dumerilii*. Brief. Funct. Genomics 12: 430–439.

Simakov, O., F. Marletaz, S. J. Cho, E. Edsinger-Gonzales, P. Havlak *et al.*, 2013b Insights into bilaterian evolution from three spiralian genomes. Nature 493: 526–531.

Smidler, A. L., O. Terenzi, J. Soichot, E. A. Levashina, and E. Marois, 2013 Targeted mutagenesis in the malaria mosquito using TALE nucleases. PLoS ONE 8: e74511.

Sodergren, E., G. M. Weinstock, E. H. Davidson, R. A. Cameron, R. A. Gibbs *et al.*, 2006 The genome of the sea urchin *Strongylocentrotus purpuratus*. Science 314: 941–952.

Srivastava, M., O. Simakov, J. Chapman, B. Fahey, M. E. Gauthier *et al.*, 2010 The Amphimedon queenslandica genome and the evolution of animal complexity. Nature 466: 720–726.

Suzuki, K. T., Y. Isoyama, K. Kashiwagi, T. Sakuma, H. Ochiai *et al.*, 2013 High efficiency TALENs enable F0 functional analysis by targeted gene disruption in Xenopus laevis embryos. Biol. Open 2: 448–452.

Takasu, Y., S. Sajwan, T. Daimon, M. Osanai-Futahashi, K. Uchino *et al.*, 2013 Efficient TALEN construction for Bombyx mori gene targeting. PLoS ONE 8: e73458.

Tessmar-Raible, K., and D. Arendt, 2003 Emerging systems: between vertebrates and arthropods, the Lophotrochozoa. Curr. Opin. Genet. Dev. 13: 331–340.

Tessmar-Raible, K., P. R. Steinmetz, H. Snyman, M. Hassel, and D. Arendt, 2005 Fluorescent two-color whole mount in situ hybridization in Platynereis dumerilii (Polychaeta, Annelida), an emerging marine molecular model for evolution and development. Biotechniques 39: 460, 462, 464.

Tessmar-Raible, K., F. Raible, F. Christodoulou, K. Guy, M. Rembold *et al.*, 2007 Conserved sensory-neurosecretory cell types in annelid and fish forebrain: insights into hypothalamus evolution. Cell 129: 1389–1400.

Tomer, R., A. S. Denes, K. Tessmar-Raible, and D. Arendt, 2010 Profiling by image registration reveals common origin of annelid mushroom bodies and vertebrate pallium. Cell 142: 800–809.

Veedin Rajan, V. B., R. M. Fischer, F. Raible, and K. Tessmar-Raible, 2013 Conditional and specific cell ablation in the marine annelid Platynereis dumerilii. PLoS ONE 8: e75811.

Wang, H., Y. C. Hu, S. Markoulaki, G. G. Welstead, A. W. Cheng *et al.*, 2013 TALEN-mediated editing of the mouse Y chromosome. Nat. Biotechnol. 31: 530–532.

Watanabe, T., H. Ochiai, T. Sakuma, H. W. Horch, N. Hamaguchi *et al.*, 2012 Non-transgenic genome modifications in a hemimetabolous insect using zinc-finger and TAL effector nucleases. Nat. Commun. 3: 1017.

Xiao, A., Z. Wang, Y. Hu, Y. Wu, Z. Luo *et al.*, 2013 Chromosomal deletions and inversions mediated by TALENs and CRISPR/Cas in zebrafish. Nucleic Acids Res. 41: e141.

Zantke, J., T. Ishikawa-Fujiwara, E. Arboleda, C. Lohs, K. Schipany *et al.*, 2013 Circadian and circalunar clock interactions in a marine annelid. Cell Rep. 5: 1–15.

Zantke, J., S. Bannister, V. B. Veedin Rajan, F. Raible, and K. Tessmar-Raible, 2014 Genetic and genomic tools for the marine annelid *Platynereis dumerilii*. Genetics 197: 19–31.

Zu, Y., X. Tong, Z. Wang, D. Liu, R. Pan *et al.*, 2013 TALEN-mediated precise genome modification by homologous recombination in zebrafish. Nat. Methods 10: 329–331.

*Communicating editor: O. Hobert*

GENETICS

**Supporting Information**
http://www.genetics.org/lookup/suppl/doi:10.1534/genetics.113.161091/-/DC1

# TALENs Mediate Efficient and Heritable Mutation of Endogenous Genes in the Marine Annelid *Platynereis dumerilii*

**Stephanie Bannister, Olga Antonova, Alessandra Polo, Claudia Lohs, Natalia Hallay, Agne Valinciute, Florian Raible, and Kristin Tessmar-Raible**


DOI: 10.1534/genetics.113.161091

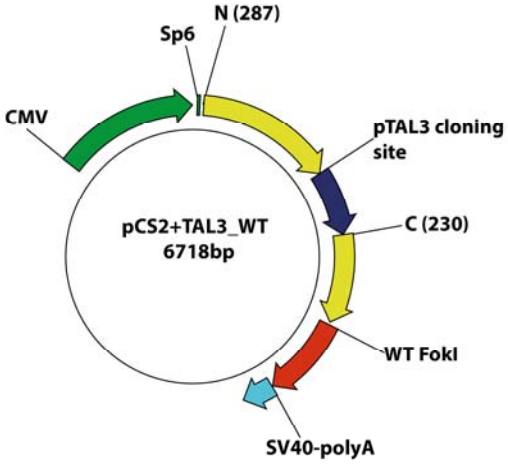


**Figure S1** Vector map of pCS2+_TAL3-WT TALEN assembly plasmid. The plasmid consists of pCS2+ backbone, which contains CMV immediate early (IE) promoter as well as Sp6 promoter for *in vitro* transcription. Regions encoding TALEN N and C terminal domains are indicated in yellow; the numbers indicate the length of the domain in amino acids. The dark blue region shows the TALEN cloning site inserted from the pTAL3 vector (Cermak et al., 2011), the red is the wildtype FokI monomeric domain and the re-inserted SV40polyA signal (from pCS2+) is shown in blue. Plasmid construction details are given in Supplementary methods.

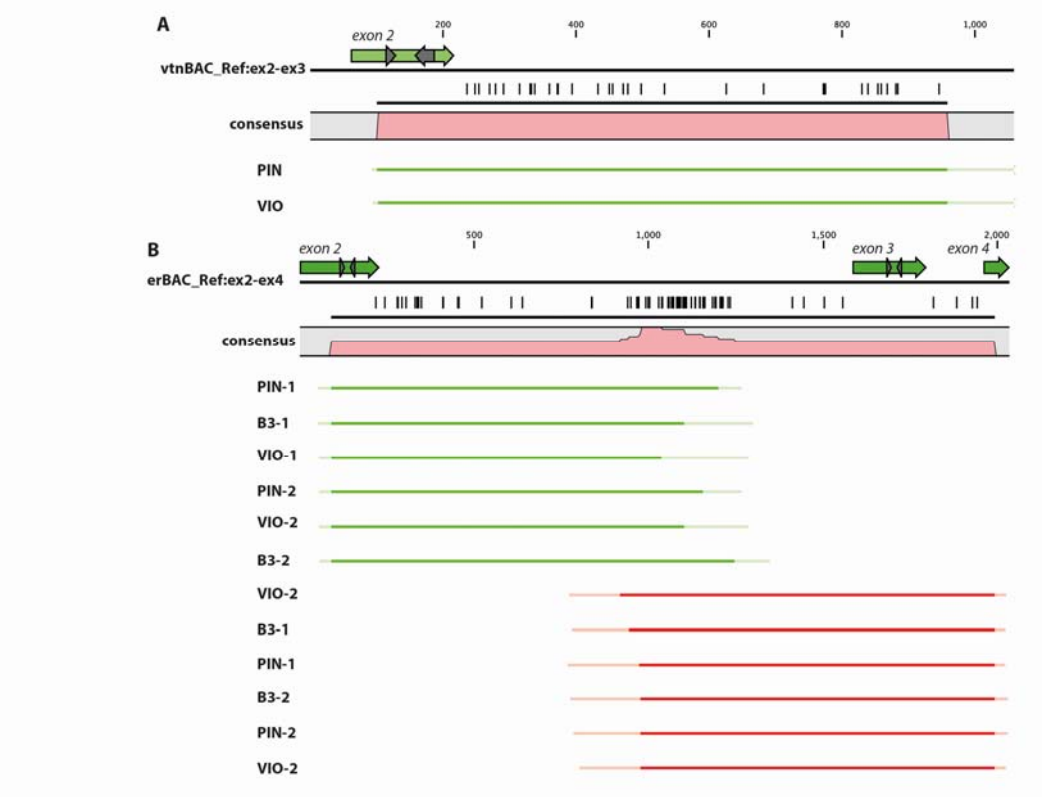


**Figure S2** Schematic of SNP positions for *vtn* and *er* genomic loci**.** CLC assemblies of sequenced genomic regions vs. BAC reference. SNPs are shown as black lines, consensus is shown by the pink graph (area under the graph/height represents degree of similarity).

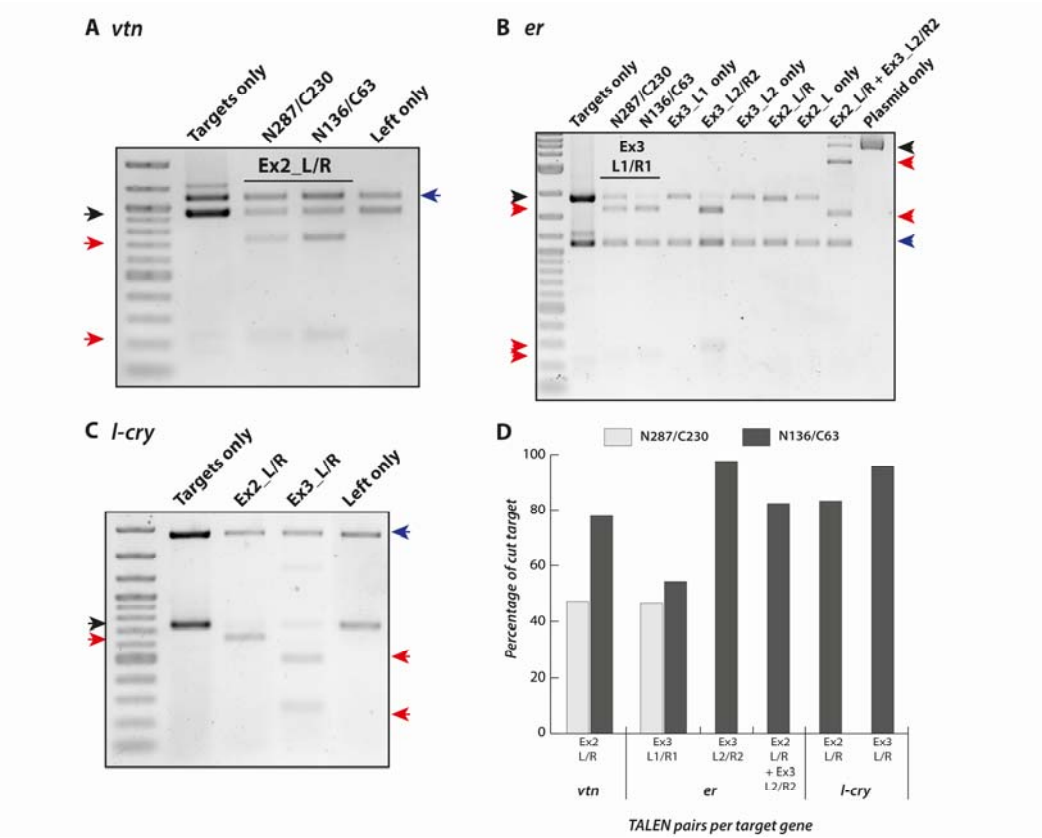


**Figure S3** Results of TnT assay for *in vitro* validation of TALEN activity. Panels (**A**) *vtn*, (**B**) *er*, (**C**) *l-cry*, (**D**) band intensity analysis quantification of cut band p*er*centage of total as measure of cleavage efficiency. Black arrows indicate size of uncut target DNA, red arrows show position of cut target DNA bands and blue arrows show position of *egfp* DNA. Ladder in each gel is 2-logDNA ladder (NEB). Negative control reactions contain Left TALEN only, other TALEN pair combinations as listed in Table S1. Alternative TALEN architectures are indicated above the lanes where compared for the same TALEN pair: N/C indicates the N or C terminal domain respectively, the numbers indicate the length of this domain in amino acids. When backbone architecture is not separately indicated: backbone is N136/C63.

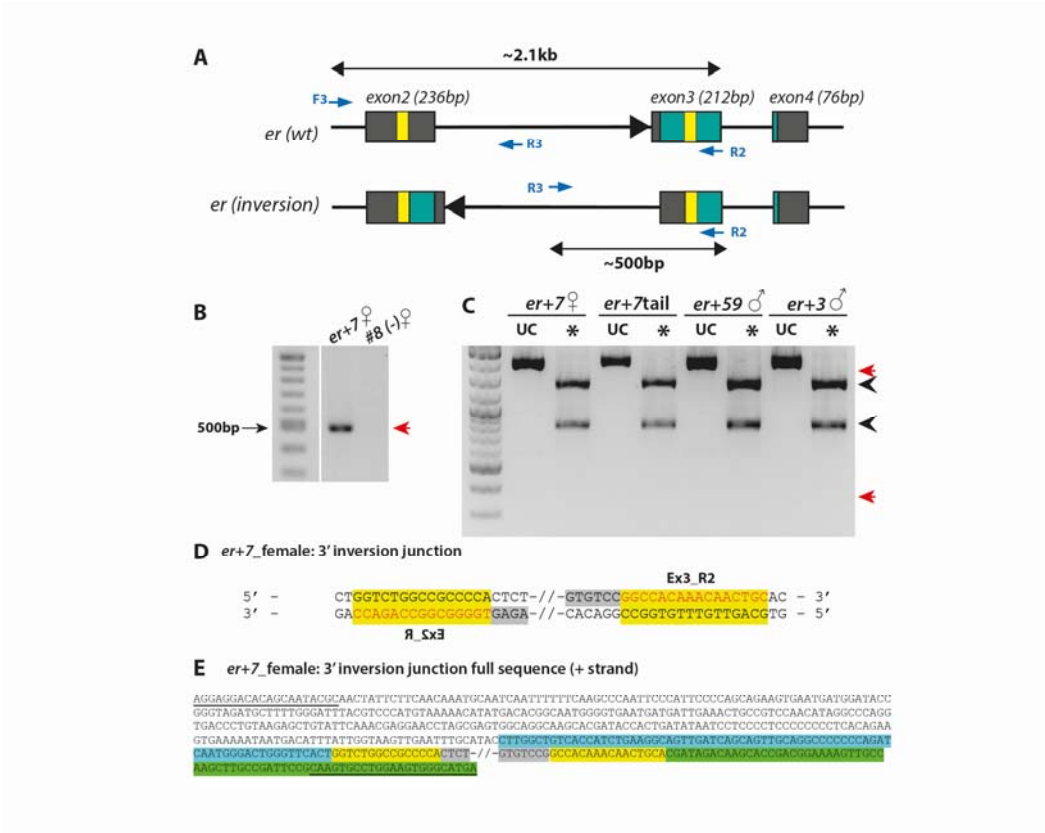


**Figure S4** Inversion resulting from simultaneous cleavage at the *er* locus. **A** Schematic of inversion and primers locations. **B** PCR result from screening with R3/R2 primers: adult TALEN-injected worms, *er+7* (insertion positive) and 8 (negative). **C)** Genomic DNA extracted from whole spawned worms: *er*+7 *er+3* and *er+59* plus gDNA from tail snip of *er+7* w*er*e screened by PCR using F3/R2 primers and digested with *Nde*I. Red arrows show position of bands expected from digestion of amplicons containing the inversion. Black arrows indicate the bands expected for digestion of wildtype amplicons. **D)** Sequence of 3' end of inversion: double stranded junction where inversion has fused spacer of exon 2 TALEN site to that of the exon 3 TALEN site. The label is reversed for the Ex2_R TALEN recognition sequence to reflect that it is now on the non-coding strand and in the opposite orientation (-). **E)** Fu**ll s**equence of 3' inversion junction: exon 2 sequence in cyan, exon 3 sequence in green, TALEN spacer in grey; TALEN recognition sites in yellow: note the sequence is the coding (+) strand, hence the inverted Ex2_R TALEN site shown is the reverse complement of the actual TALEN binding sequence.

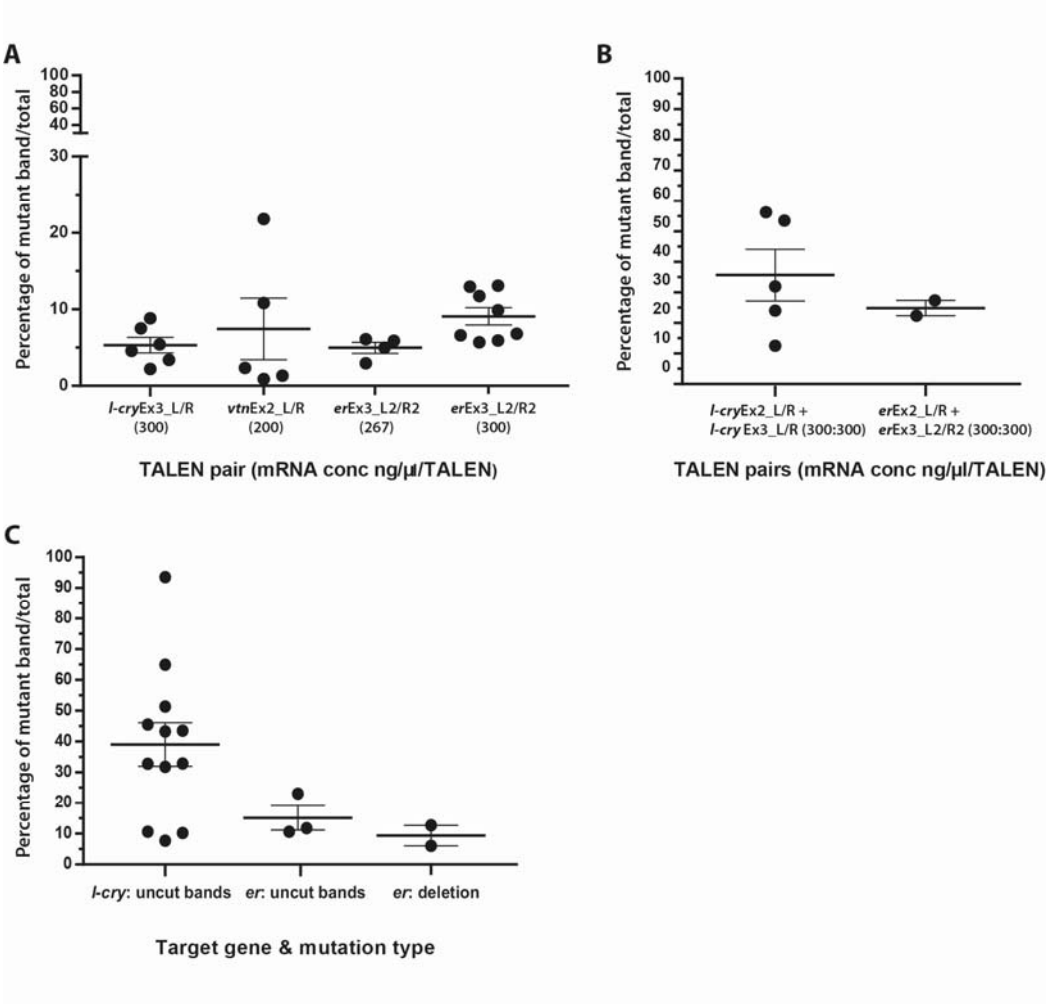


**Figure S5** Individual mutation rates for larvae and adult TALEN-injected worms. The percentage of mutant bands (i.e. uncut, or short bands representing deletions) of the total PCR product was used to infer the mutation rates for individual larval samples and adult worms. **A)** Percentage of uncut band detected in injected larval samples (pools of 4 larvae/sample). **B)** Percentage of deletion bands in total PCR product in pooled larval samples. mRNA concentration(s) of TALENs in brackets. **C)** Percentage of uncut/deletion bands out of total for individual adult worms. The *l-cry* uncut bands were detected at the exon 3 site via *Ava*II digestion (see Fig. 3), *er* uncut bands were detected at exon 3 site via *Afl*III digestion (see Fig. 2), *er* deletions represented are those detected for *er+32* and *er+59*. Each dot represents the percentage of mutant band calculated from a single sample. Bold lines indicate the mean % of mutant band and whiskers indicate the standard deviation. See also Tables 1 and 2.

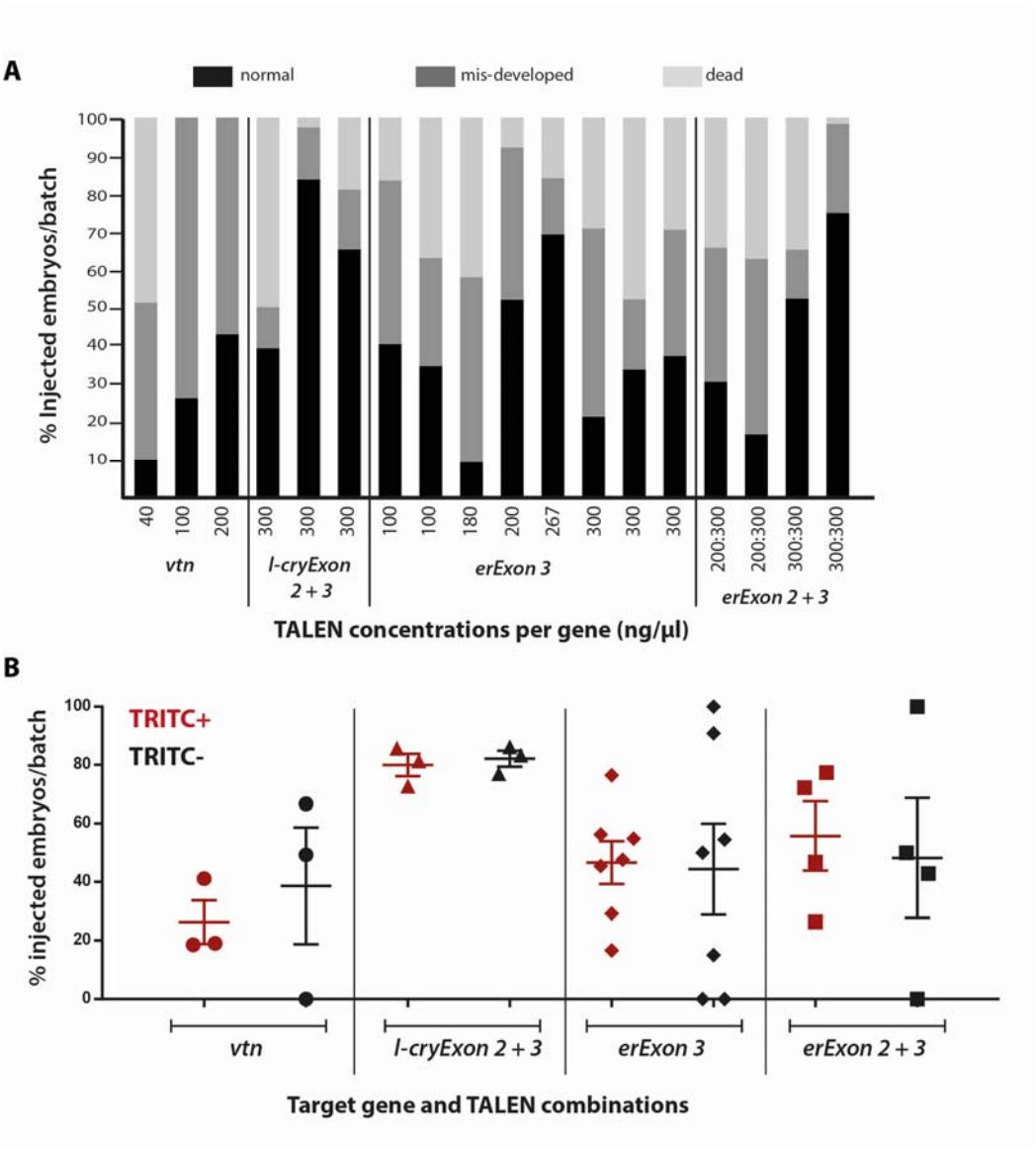


**Figure S6** Survival data for TALEN injected embryos**. A)** Rates of dead (light grey), misdeveloped (dark grey) and normal (black) larvae from TALEN injections. Each bar represents an individual injection batch. The *x* axis indicates the target gene and exon; numbers indicate the concentration of TALEN mRNA (ng/ul/TALEN). **B)** Survival of injected larvae at 24hpf. Embryos were sorted based on TRITC fluorescence: TRITC+ = injection-positive; TRITC- = injection-negative. Each dot represents the survival of larvae from a single injection batch.

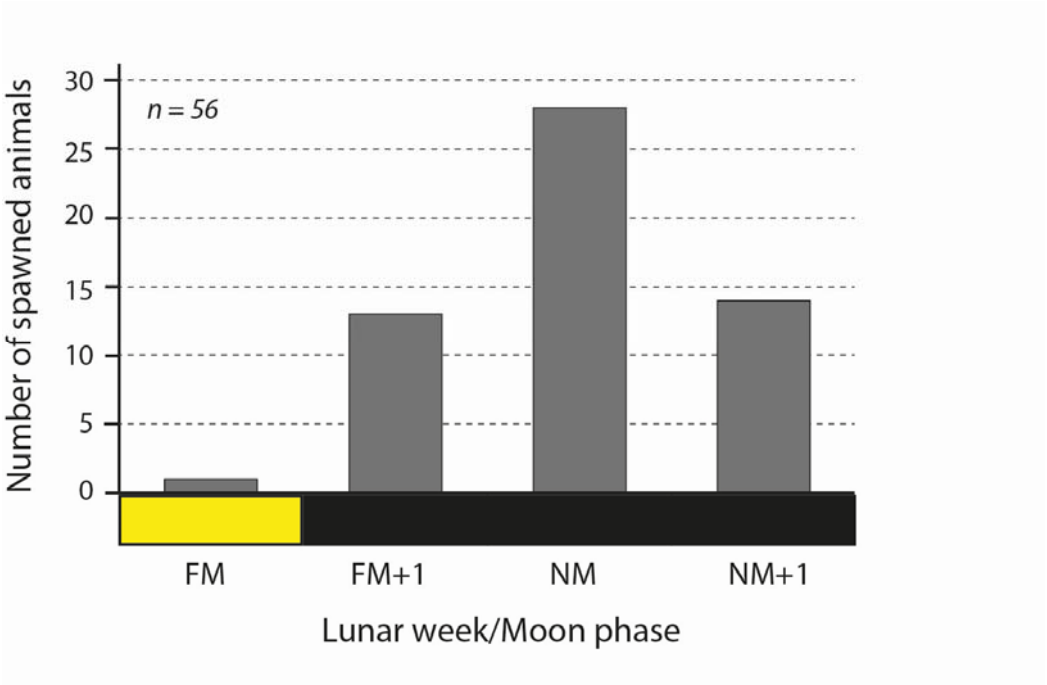


**Figure S7** Spawning graphs and batch survival data for mature TALEN-injected worms. Spawning data for TALEN-injected mature worms. Spawning data is plotted according to moon phases and arranged by lunar week: NM = new moon, FM = full moon +1 indicates the week after either NM (NM+1) or FM (FM+1), yellow indicates nocturnal illumination during FM week, black indicates no nocturnal illumination during non-FM weeks (see (ZANTKE *et al.* 2013) for details).

**File S1**

**Supplementary Methods**

**Recombinant DNA techniques and sequencing.**

Ligations, transformations and plasmid purifications were performed according to standard protocols (GREEN and SAMBROOK 2012).

TALEN assembly plasmids (steps 1 and 2 products) were sequenced using the primers indicated in the GoldenGate kit protocol. The pJET1.2-fow and –rev primers were used to sequence subclones in the pJET1.2 backbone. Sequence alignments were performed using CLC Main Workbench (v.6.6.1 onwards, CLC bio).

**Construction of pCS2+_TAL3-WT TALEN expression vector**

A pTAL3 vector containing a full length RVD array with *Bgl*II and *Apa*I, to liberate the entire TALEN-encoding sequence from start of N-terminal sequence to end of FokI. The digested fragment was gel purified (Qiagen Gel Extraction kit) and ligated into the pCS2+ expression vector backbone: cut with *Bam*HI/*Apa*I. The resulting vector, called pCS2+_TALEN-WT, lacked a polyA signal, due to removal during the *Bam*HI/*Apa*I digest. The SV40 polyA signal was re-inserted by first amplifying this sequence from original pCS2+ using PCR primers that added 5' *Sac*I and 3' *Kpn*I restriction sites and ligated into the pCS2+_TALEN-WT vector backbone cut with the same enzymes.

The resultant vector pCS2+_TALEN-WT-pA was then modified to replace the TALEN RVD array with the cloning site from the pTAL3 vector from the GoldenGate TALEN Assembly kit (v1.0: (CERMAK *et al.* 2011)). Both pCS2+_TALEN-WT-pA and pTAL3 were digested with BamHI. The vector band of the cut pCS2+TALEN-WT-pA and the cut *Bam*HI fragment from pTAL3 were gel purified and then ligated together to form the final pCS2+_TAL3-WT vector.

**Genotyping to identify allelic variants and SNPs in genes targeted for modification using TALENs**

Genomic PCR was carried out using 25 µl or 50 µl final volumes, with 1µl of gDNA (diluted 1:10-1:50 to approx. 10-20 ng total DNA), forward and reverse primers (0.2 µM ea.), dNTPs (0.4 mM) and Phusion polymerase (Fermentas). PCR cycles: 98°/30 s; 35x[98°/30 s; 62°/1 min; 72°/1 min/kb].

**Establishing a protocol for rapid assessment of TALEN functionality.**

The small size of *Platynereis* larvae precluded kit-based methods to obtain genomic DNA from single or small-pools of injected larvae for screening. We tested a rapid method for preparing genomic DNA extracts from single, or small pools of larvae (24hpf or older). To maximize compatibility with PCR screening assays, we used 1X PCR

buffer (Qiagen, HotStar Taq Plus kit), supplemented with 1volume of proteinase K (22 mg/ml stock) per 10 volumes of buffer. This buffer was sufficient for digesting small numbers of pooled larvae at 24 hpf, or single larvae from 3 days post fertilisation to 1 month old juveniles.

To collect embryos for digestion, 1-5 embryos were collected in a 0.2 ml PCR tube and kept on ice until all embryo samples are collected. As much NSW was removed from the collected embryos before Digestion buffer was added. For single larvae we used 5-10 µl, for pools of 2 larvae: 10-20 µl and for pools of 3 or more larvae we used 30-50 µl. It was possible to use lysate prepared from mis-developed embryos, although amplification tended much less efficient. Using 1-2 µl of larval lysate was sufficient to achieve PCR amplification for the assays described below. Samples were stored at 4°C for up to 2 weeks, or for longer at -20°C.

**Amplification of target DNA for TnT assay**

Targets for TnT assay were amplified either from genomic DNA (*l-cry* and *er*) or cDNA (*vtn*). Primers for TnT target amplification were: *l-cry*F1/R1; *er*F1/R1; *vtn*F2/R2 (970 bp). PCR products were purified by first pooling PCR products from 4 replicate reactions together and extracting using Qiagen MinElute kit (Qiagen), or Gel Extraction Kit (Qiagen).

**Phenol-chloroform extraction of TnT assay reaction products**

Following incubation of TnT reactions, the volume was adjusted to 200µl using nuclease-free water and added to the phase-lock tube. An equal volume of phenol:chloroform:isoamyl alcohol (25:24:1, AppliChem) was added and samples mixed. Samples were centrifuged at 12,000 x g for 5 minutes and the aqueous phase was extracted a second time with an equal volume of chloroform. DNA was precipitated from the aqueous phase using 300 µl 100% ethanol and 10 µl 3 M sodium acetate (pH5.2) at -20° for 30 minutes, followed by centrifugation at 20,000 x g for 15 minutes in a refrigerated microcentrifuge. The DNA pellet was washed once with ice cold 70% ethanol with centrifugation as above. The pellet was air-dried and resuspended in 8 µl of nuclease-free water + 2 µl RNase A (1:1000 dilution in P1 buffer Qiagen Midiprep kit), incubated at room temperature for 5 minutes.

**List of Primer sequences**

*vtn*F1 (1806) ATGCAATTTTCGCGGCCCACCTTC

*vtn*R1 (1807) CAGATTCTAACGTGTTA$^{AT}$GTAGCATCC

*vtn*F2 (1826):GAAGTGCCGTAGTTCGCGCTGC

*vtn*R2 (1827):GATGCATGACATAGTCAAATGAACAAATGTTG

*vtn*R3 (2364): AGTTTGCACCCAGCCATGGTC

*er*F1 (1063): ATGGCAGACGACAGCCAAGGG

*er*R1 (Ex3R: 2365): TTCTTTGTTGTCCGCCTTTC

*er*F2 (F3: 2366): ATTGCCATGTCCTCCTCCTG

*er*R2 (Ex2R: 2367): TCATGCCCACTTCCAGGCACTTG

*er*F3 (L2R2F: 2368): CTGGGAACAAAGAGGCTGAG

*er*R3 (L2R2R: 2369): AGGAGGACACAGCAATACGC

*l-cry*F1 (up2: 2370): ACTTTTGAGCAGTGAATAACTGA

*l-cry*R1 (D: 2371) : TTGTCATACCTCAATCAGCT

*Sac*I-5'-polyA (2362): 5' - TAATAGGAGCTCGCAGACATGATAAGATACATTGATG – 3';

*Kpn*I-3'-polyA (2363):5' - AAGCTGGGTACCGTACCACATTTGTAGAGGTTTTAC – 3'

**Table S1 TALEN pairs reported in this study**

| Gene | TALEN pair | Left TALEN RVDs | Right TALEN RVDs | Target sequence (+ strand)[a] |
|---|---|---|---|---|
| *er*/exon2 | *er*Ex2_L/_R | NG NI HD NI HD HD HD HD NG HD NI NN NI NN NI | NN NN NG HD NG NN NN HD HD NN HD HD HD HD NI | TTACACCCCTCAGAGAtctccagaagaagagTGGGGCG GCCAGACCA |
| *er*/exon3 | *er*Ex3_L1/_R1 | HD HD NN NN HD HD NI HD NI NI NI HD NI NI HD NG | HD NN NN HD NI NI NN HD NG NG NN NN HD NI NI HD NG NG NG NG | TCCGGCCACAAACAACTgcacgatagacaagcaccgacgg AAAAGTTGCCAAGCTTGCCGA |
| *er*/exon3 | *er*Ex3_L2/_R2 | NG NG NN HD NI NI NN NN HD HD HD HD NN NG NN | NN HD NI NN NG NG NN NG NG NG NN NG NN NN HD | TTTGCAAGGCCCCGTGgattacgtgtgtccgGCCACAAA CAACTGCA |
| *l-cry*/exon2 | *l-cry*Ex2_L/_R | HD NG NG NG NN NN HD NG HD HD NG NG HD HD NI | NG NN HD NI NG NN NI HD NI NI NG HD HD NG NN | TTGCATGACAATCCTGctctgctcaagtcccTGGAAGGA GCCAAAGA |
| *l-cry*/exon3 | *l-cry*Ex3_L/_R | NI HD NG NN NN NI NN NG NN NG HD NG NI NI NI | HD HD NI NG NN HD NG NG HD NG NG HD NI NI NI | TACTGGAGTGTCTAAAggaccttgatgacagTTTGAAGA AGCATGGA |
| *vtn*/exon2 | *vtn*Ex2_L/R | NN NG NG NG NN NG NG NN NG NG HD NN NN HD HD NG | NI NN NI NI HD NN NG NG NG NN HD HD HD HD HD NG | TGTTTGTTGTTCGGCCTgttttgttcgcaattgtccaccaGG GGGCAAACGTTCTA |

[a] 5′ T preceding TALEN binding sequence is und*er*lined, TALEN recognition sites are in upper case, spacer sequence in lower case. The sequence is of the sense strand, hence the right TALEN binds the rev*er*se complement of the sequence shown.

**Table S2 PCR and restriction digest assays for *in vivo* genotyping and mutation screening:**

| Gene & TALEN pair | Forward primer | Reverse primer | PCR size (bp) | Restriction Site | Cut band sizes (WT) |
|---|---|---|---|---|---|
| *er*Ex2_L/_R | F3 | R3 | 915 | BpmI | 446; 469 |
| *er*Ex3_L1/_R1 | F2 | R2 | 479 | Hpy99I | 426; 53 |
| *er*Ex3_L2/_R2 | F2 | R2 | 479 | AflIII | 387; 92 |
| *er*Ex2_L/R + *er*Ex3_L2/R2 (deletion)[a] | F1 | R1 | WT: ~1900<br>Del: ~380 | NA | NA |
| *er*Ex2_L/R + *er*Ex3_L2/R2 (deletion) | F3 | R2 | WT: ~2100<br>Del: ~700 | NdeI (inversion) | WT:<br>Inv.: |
| *er*Ex2_L/R + *er*Ex3_L2/R2 (inversion) | R3 | R2 | ~600 | NA | NA |
| *l-cry*Ex2_L/R[a] | F1 | R1 | 729 | SmoI | 482; 247 |
| *l-cry*Ex2_L/R[a] | F1 | R1 | 729 | AvaII | 633; 96 |
| *l-cry*Ex2_L/R + *l-cry*Ex3_L/R | F1 | R1 | WT: 729<br>Del: ~320 | NA | NA |
| *vtn* genotyping[a] | F1 | R1 | | | |
| *vtn*Ex2_L/R | F1 | R3 | 257 | MfeI | 167; 90 |

[a] also used for genotyping and amplification of target DNA for *in vitro* TnT cleavage assay.

**Table S3 Mapped Single Nucleotide Polymorphisms for *er* and *vtn* genomic loci**

| | nucleotide position | Ref: Allele A | PIN: Allele B | B3: Allele C |
|---|---|---|---|---|
| vtn intron 2 | 236 | A | C | |
| | 248 | C | T | |
| | 254 | A | G | |
| | 270 | C | C | |
| | 279 | A | G | |
| | 291 | T | T | |
| | 315 | G | T | |
| | 331 | G | G | |
| | 333 | A | T | |
| | 338 | A | G | |
| | 360 | A | G | |
| | 372 | A | G | |
| | 373 | T | T | |
| | 394 | G | T | |
| | 433 | C | T | |
| | 450 | T | T | |
| | 455 | C | T | |
| | 471 | A | G | |
| | 478 | A | G | |
| | 498 | G | G | |
| | 533 | T | T | |
| | 626 | A | G | |
| | 682 | A | G | |
| | 772 | T | T | |
| | 774 | C | T | |
| | 775 | A | T | |
| | 830 | T | T | |
| | 839 | G | G | |
| | 854 | G | G | |
| | 859 | C | T | |
| | 868 | G | T | |
| | 881 | G | G | |
| | 884 | T | T | |
| | 946 | G | T | |
| er exon 2 | 219 | T | C | C |
| er intron 2 | 245 | A | C | C |
| | 280-281 | - | + A | + A |
| | 282 | A | G | G |
| | 292-293 | - | + C | + C |
| | 304 | A | C | C |
| | 330 | C | A | A |
| | 336 | A | G | G |
| | 340 | T | C | C |
| | 348 | T | A | A |
| | 410 | T | T | T |
| | 411 | T | T | T |
| | 453 | A | C | C |
| | 456 | A | - | - |
| | 522 | T | A | A |
| | 607 | G | T | G |
| | 639 | A | T | T |
| | 838 | C | - | - |

| | | | | |
|---|---|---|---|---|
| | 839 | T | - | - |
| | 1067 | A | G | G |
| | 1073 | T | C | C |
| | 1084 | C | T | T |
| | 1207 | C | T | T |
| | 1210 | G | A | A |
| | 1231 | C | A | A |
| | 1410 | C | G | G |
| | 1443 | C | T | T |
| | 1502 | A | A | T |
| | 1555 | T | T | A |
| er intron 3 | 1816 | C | C | T |
| | 1883 | G | G | C |
| | 1928 | G | G | T |
| | 1942 | T | T | G |

**Table S4 Survival data for TALEN injected worms as percentage**

| gene | TAL pair | conc | % dead | % live | % TRITC+ | % TRITC- | TRITC+ 24hpf % normal | % mis dev. | TRITC- 24hpf % normal | % mis dev. | % survival rates 48 hpf | 72 hpf | 96hpf | adult* |
|---|---|---|---|---|---|---|---|---|---|---|---|---|---|---|
| **vtn** | **Ex2_L/R** | 40 | 48.78 | 51.22 | 100.00 | 0.00 | 19.05 | 80.95 | 0.00 | 0.00 | NA | NA | NA | |
| | | 100 | 0.00 | 100.00 | 84.33 | 15.67 | 18.58 | 81.42 | 66.67 | 33.33 | NA | NA | NA | |
| | | 200 | 0.00 | 100.00 | 79.34 | 20.66 | 41.13 | 58.87 | 49.28 | 50.72 | NA | NA | 18.35 | 65.00 |
| **lcry** | **Ex2_L/R + Ex3_L/R** | 300 | 50.00 | 50.00 | 47.83 | 52.17 | 72.73 | 27.27 | 83.33 | 16.67 | NA | NA | 91.67 | 77.57 |
| | | 300 | 2.40 | 97.60 | 64.42 | 35.58 | 85.71 | 14.29 | 86.21 | 13.79 | NA | NA | 55.56 | |
| | | 300 | 18.84 | 81.16 | 76.79 | 23.21 | 81.40 | 18.60 | 76.92 | 23.08 | NA | NA | 100.00 | |
| **er** | **Ex3_L2/R2** | 100 | 16.46 | 83.54 | 91.97 | 8.03 | 47.62 | 52.38 | 54.55 | 45.45 | NA | NA | NA | |
| | | 100 | 27.03 | 72.97 | 62.96 | 0.00 | 54.90 | 45.10 | ND | ND | NA | NA | NA | |
| | | 180 | 42.11 | 57.89 | 54.55 | 45.45 | 16.67 | 83.33 | 15.00 | 85.00 | 0.00 | 0.00 | 0.00 | |
| | | 200 | 7.14 | 92.86 | 92.31 | 0.00 | 56.25 | 43.75 | ND | ND | NA | NA | NA | |
| | | 267 | 15.79 | 84.21 | 60.71 | 39.29 | 76.47 | 23.53 | 90.91 | 9.09 | NA | NA | NA | |
| | | 300 | 29.09 | 70.91 | 96.58 | 3.42 | 29.20 | 70.80 | 50.00 | 50.00 | 3.03 | 3.03 | 3.03 | 75.00 |
| | | 300 | 47.96 | 52.04 | 64.71 | 35.29 | 45.45 | 54.55 | 100.00 | 0.00 | 13.33 | 13.33 | 6.67 | |
| | | 400 | 29.41 | 70.59 | 100.00 | 0.00 | 52.78 | 47.22 | ND | ND | 15.79 | 15.79 | 0.00 | |
| | | 400 | 21.88 | 78.13 | 80.00 | 20.00 | 68.33 | 31.67 | 80.00 | 20.00 | 73.17 | 73.17 | 14.63 | |
| **er** | **Ex2_L/R + Ex3_L2/R2** | 200:300 | 34.38 | 65.63 | 91.67 | 8.33 | 46.75 | 53.25 | 42.86 | 57.14 | 91.67 | 91.67 | 41.67 | 64.52 |
| | | 300:200 | 37.28 | 62.72 | 100.00 | 0.00 | 26.42 | 73.58 | ND | ND | 53.57 | 53.57 | 3.57 | |
| | | 300:300 | 34.84 | 65.16 | 71.29 | 28.71 | 72.22 | 27.78 | 100.00 | 0.00 | 57.69 | 57.69 | 32.69 | |
| | | 300:300 | 1.47 | 98.53 | 95.52 | 4.48 | 77.34 | 22.66 | 50.00 | 50.00 | NA | NA | 60.61 | |

**References**

Cermak, T., E. L. Doyle, M. Christian, L. Wang, Y. Zhang *et al.*, 2011 Efficient design and assembly of custom TALEN and other TAL effector-based constructs for DNA targeting. Nucleic Acids Res 39**:** e82.

Green, M. R., and J. Sambrook, 2012 *Molecular Cloning: A Laboratory Manual* Cold Spring Harbor Laboratory Press.

Zantke, J., T. Ishikawa-Fujiwara, E. Arboleda, C. Lohs, K. Schipany *et al.*, 2013 Circadian and Circalunar Clock Interactions in a Marine Annelid. Cell Reports 5**:** 99-113.